SUPPLEMENTARY MATERIALS

Novel correlations between spectroscopic and morphological properties of activated carbons from waste coffee grounds

*Egle Rosson, Paolo Sgarbossa, Mirto Mozzon, Federico Venturino, Sara Bogialli, Antonella Glisenti, Aldo Talon, Elisa Moretti, Sara Carturan, Sergio Tamburini, Alessia Famengo, Ana Paula da Costa Ribeiro, Sadjia Benhabiles, Rida Kamel, Federico Zorzi, and Roberta Bertani**

List of supplementary Figures and Tables:

- Figure S10. Selected N_2 absorption isotherm profiles together with pore size distribution.

- Figure S11. ESEM images of the activated carbons at different magnifications.

- Figure S12. TEM images of the samples AAC-5, AAC-6, and AAC-7, prepared by KOH activation at 600°C, 700°C and 800°C, respectively.

- Figure S13. (a): Raman I_D/I_G ratio *vs* pore diameter for samples with BET values higher than 1000 m^2/g. **(b):** Raman I_D/I_G ratio *vs* pore diameter for samples with BET values lower than 1000 m^2/g.

- Figure S14: Raman I_D/I_G ratio *vs* specific surface area for samples with BET values higher than 1000 m^2/g.

Figure S1. ESEM data of the starting SCGs.

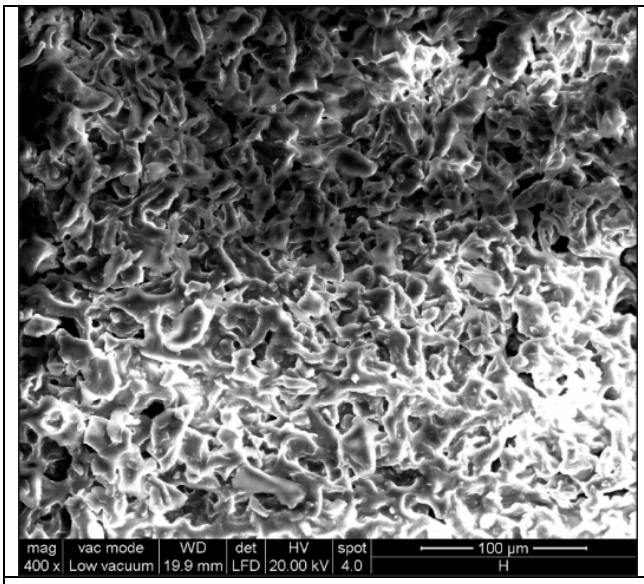

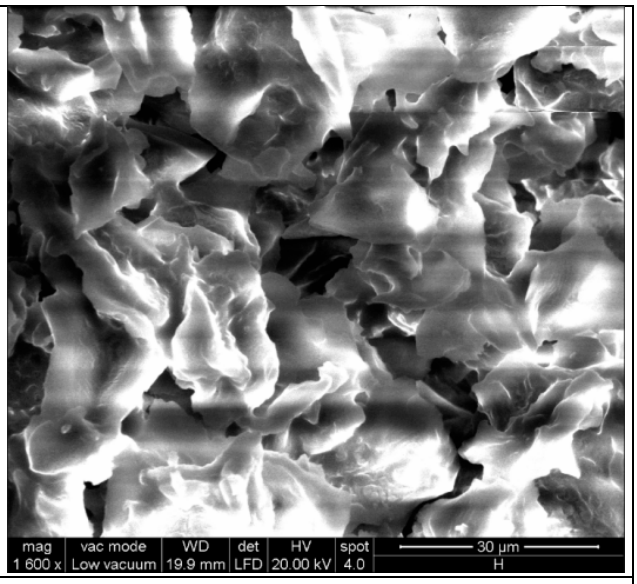

(a): ESEM image at 400X and at 1600X of a typical sample of the starting Robusta coffee grounds (dark brown flakes)

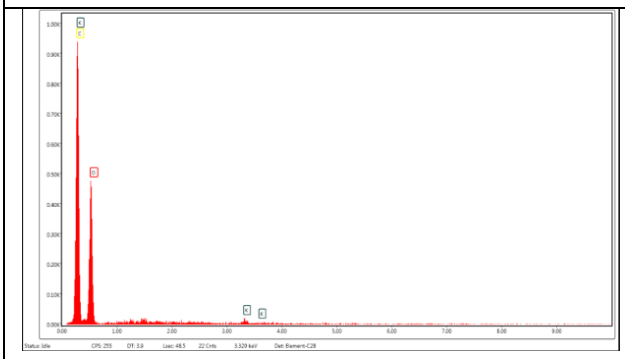

XRF analysis: the data correspond to averaged values of five independent samples

Element	w/w %	Atomic %
C	52.7	59.9
O	46.9	40.0
K	0.4	0.1

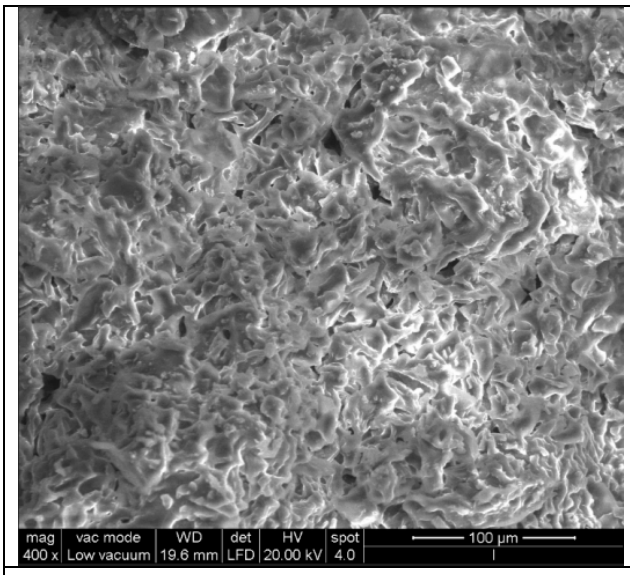

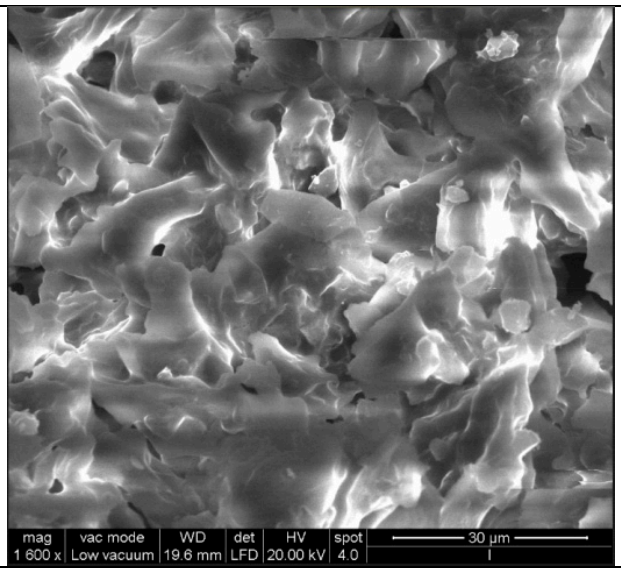

(b): ESEM image at 400X and 1600X of a typical sample of the starting Arabica coffee grounds (light brown, more compact, flakes)

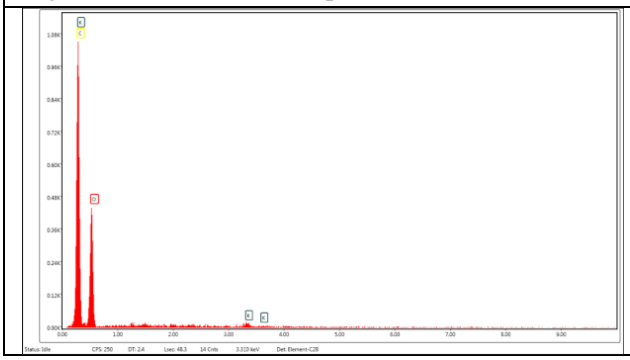

XRF analysis: the data correspond to averaged values of at least three measurements on five independent samples

Element	w/w %	Atomic %
C	55.9	63.0
O	43.5	36.8
K	0.6	0.2

Figure S2. GC MS analysis of the EtOH mother liquors after washing spent coffee grounds from Arabica.

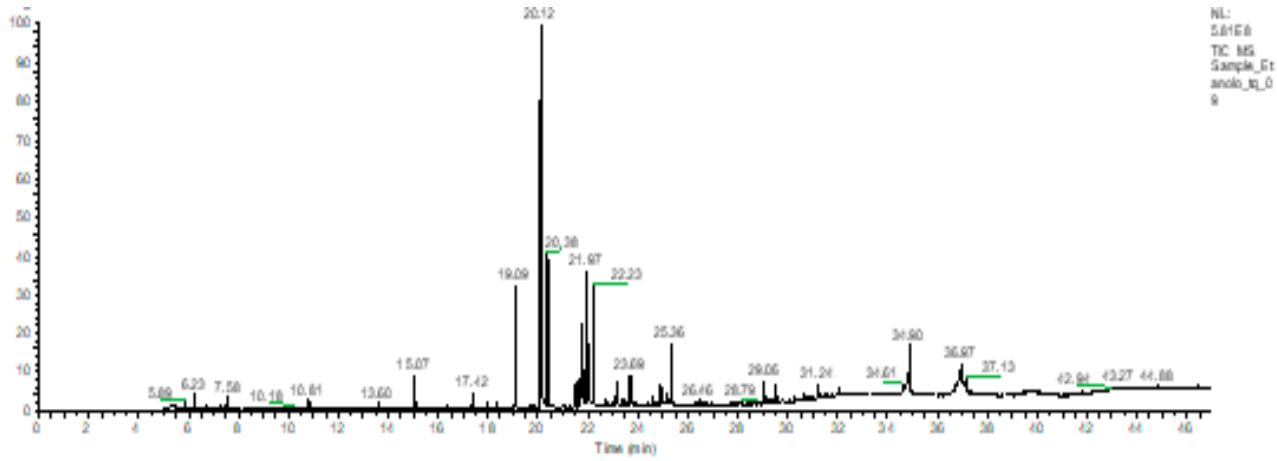

Retention time (min)	Some peaks identification according to library
15.07	N,N-dimethyl dodecanamine
19.09	Caffeine
20.12	Hexadecanoic acid (C16)
20.36	Hexadecanoic acid methyl ester
21.97	Octadecanoic acid (C18)
22.23	15-methyl-heptadecanoic acid ethyl ester
23.09	Icosanoic acid (C20)
25.30	9,11-octadiene acid ethyl ester
34.90	Hexadecanoic acid ethyl ester

Figure S3. (a). ^{13}C HPDEC NMR spectrum in the solid state of caffeine. (b). ^{13}C HPDEC NMR in the solid state of R and A samples.

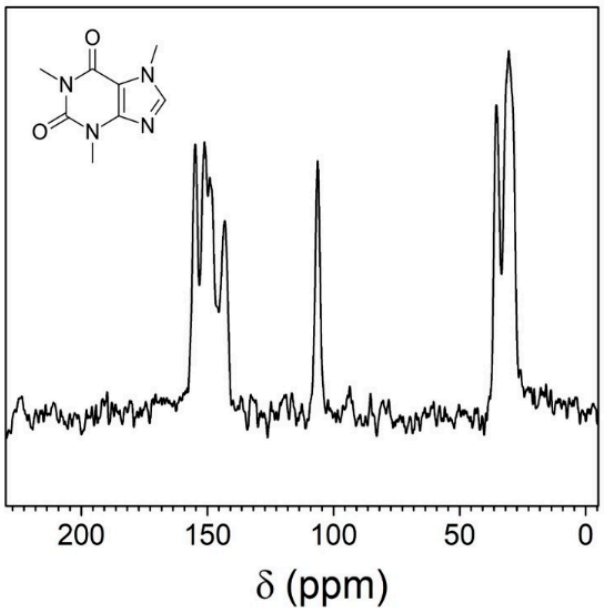

(a)

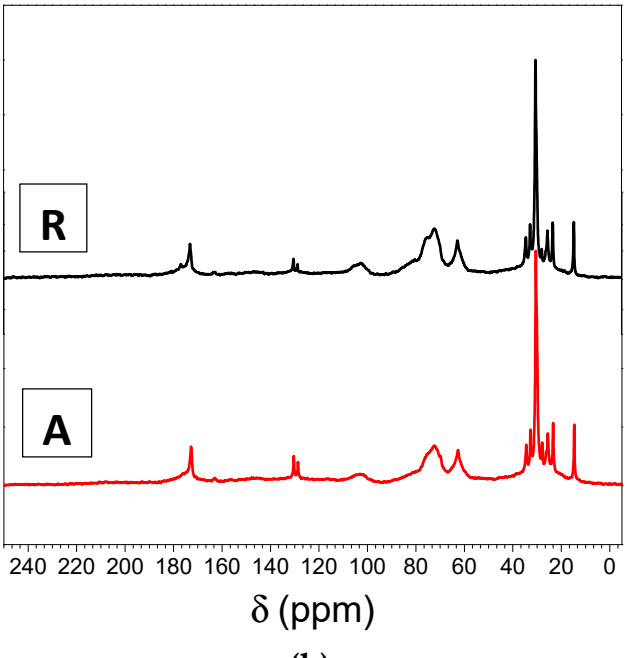

(b)

Table S1. ^{13}C MAS Chemical shifts.

A	172.8	130.4	128.7	102.4 (br)	72.4 (br)	62.6 (br)	34.4	32.7	30.5	27.9	25.6	23.4	14.7
R	173.0	130.4	128.7	102.4 (br)	72.1 (br)	62.7 (br)	34.5	32.7	30.5	27.9	25.6	23.4	14.7

Figure S4. TG and DTG profiles of R and A under air.

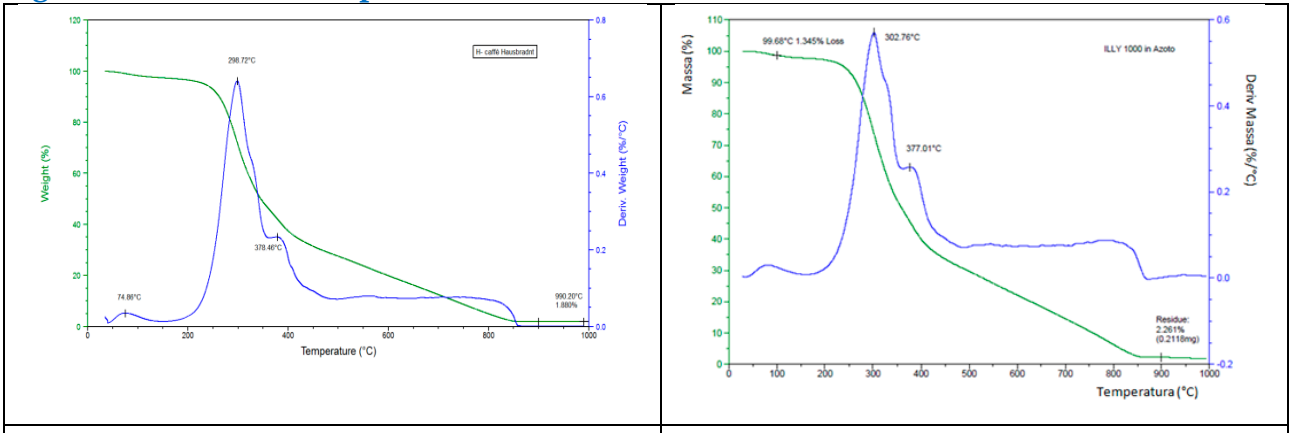

(a): TG and DTG profile of sample **R** in the range 30-920°C (10°C/min) under air

(b): TG and DTG profile of sample **A** in the range 30-920°C (10°C/min) under air

Both samples showed, under air, from room temperature to 100°C the release of residual moisture (ca. 5% at about 75°C). In the range from 200°C to 400°C a weight loss of about 60% could be observed followed by a progressive weigth loss until final residue of about 2% w/w.

Table S2: TG and DTG data of samples A, R, A/KOH, and R/KOH 1/1 mixtures in the range 30-1000°C under nitrogen.

Sample	**T** (°C)	**Weight loss** (%)	**Combined weight loss** (%)	**Notes**
A	108	3		moisture loss
	298	32	72	emicellulose decomposition
	332	5		cellulose decomposition
	389	35		lignine decomposition
				final residue = 22.76%
R	95	4		moisture loss
	300	25	70	emicellulose decomposition
	334	10		cellulose decomposition
	384	35		lignine decomposition
				final residue = 23.01%
A/KOH	101	5		moisture loss and H_2 evolution
	166	3	20	
	199	3		C_2 hydrocarbons, CH_4 and H_2O evolution
	214-225	9		
	288	5		
	380-450	15		CO, CO_2, CH_4, C_2H_6, C_2H_4 evolution
	600-800	10		carbonization
	900	20		final residue = 31.44%
R/KOH	94	15		moisture loss and H_2 evolution
	280	15		C_2 hydrocarbons, CH_4 and H_2O evolution
	377-410	15		CO, CO_2, CH_4, C_2H_6, C_2H_4 evolution
	600-800	10		carbonization

900	10	final residue = 35.04%

Figure S5. (a). GC MS analysis of the acetone solution of the residue after treatment at 380°C for 6 h under nitrogen of a 1:1 mixture A:KOH. (b). ESEM images of the black powder recovered from treatment at 380°C for 6 h under nitrogen of a 1:1 mixture A:KOH.

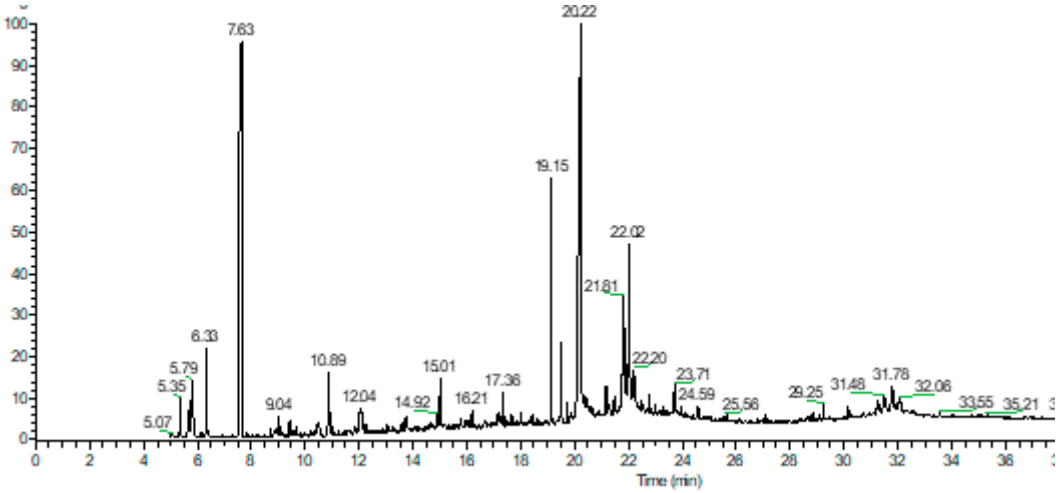

Retention time (min)	Some peaks identification according to library
7.63	3-ethoxy propanoic acid ethyl ester
19.15	Caffeine
20.22	Hexadecanoic acid methyl ester
21.81	Octadecanoic acid methyl ester
22.02	Octadecanoic acid ethyl ester

(a)

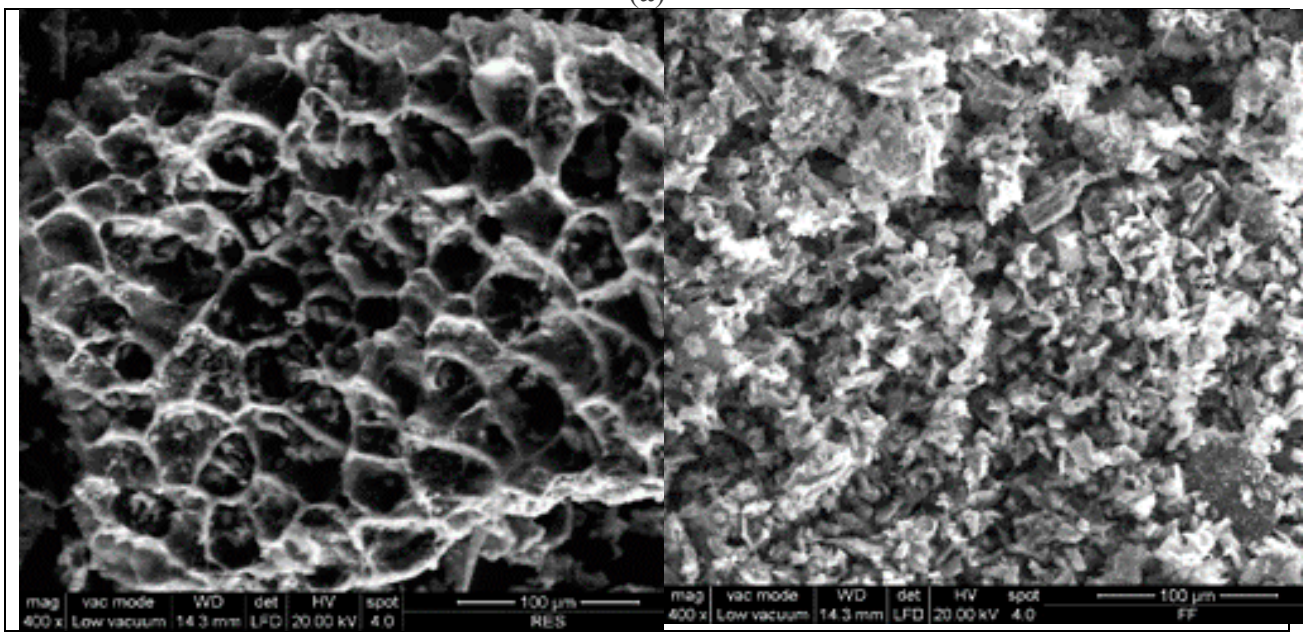

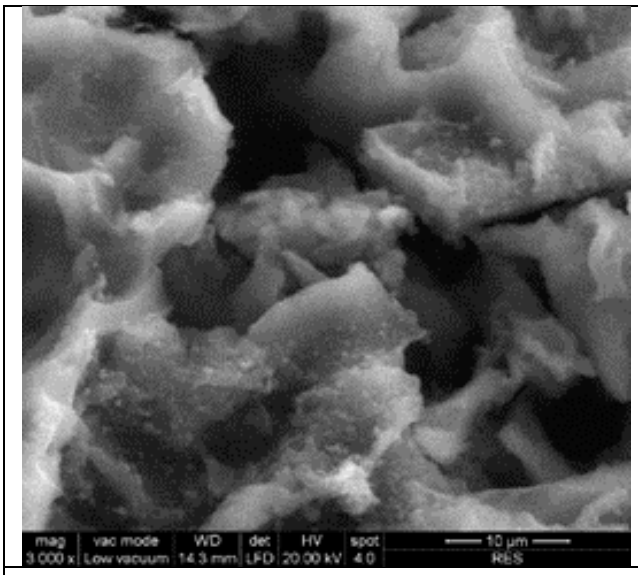

Spongy fraction | Powder fraction

(b)

Figure S6. Raman spectra of the prepared activated carbons.

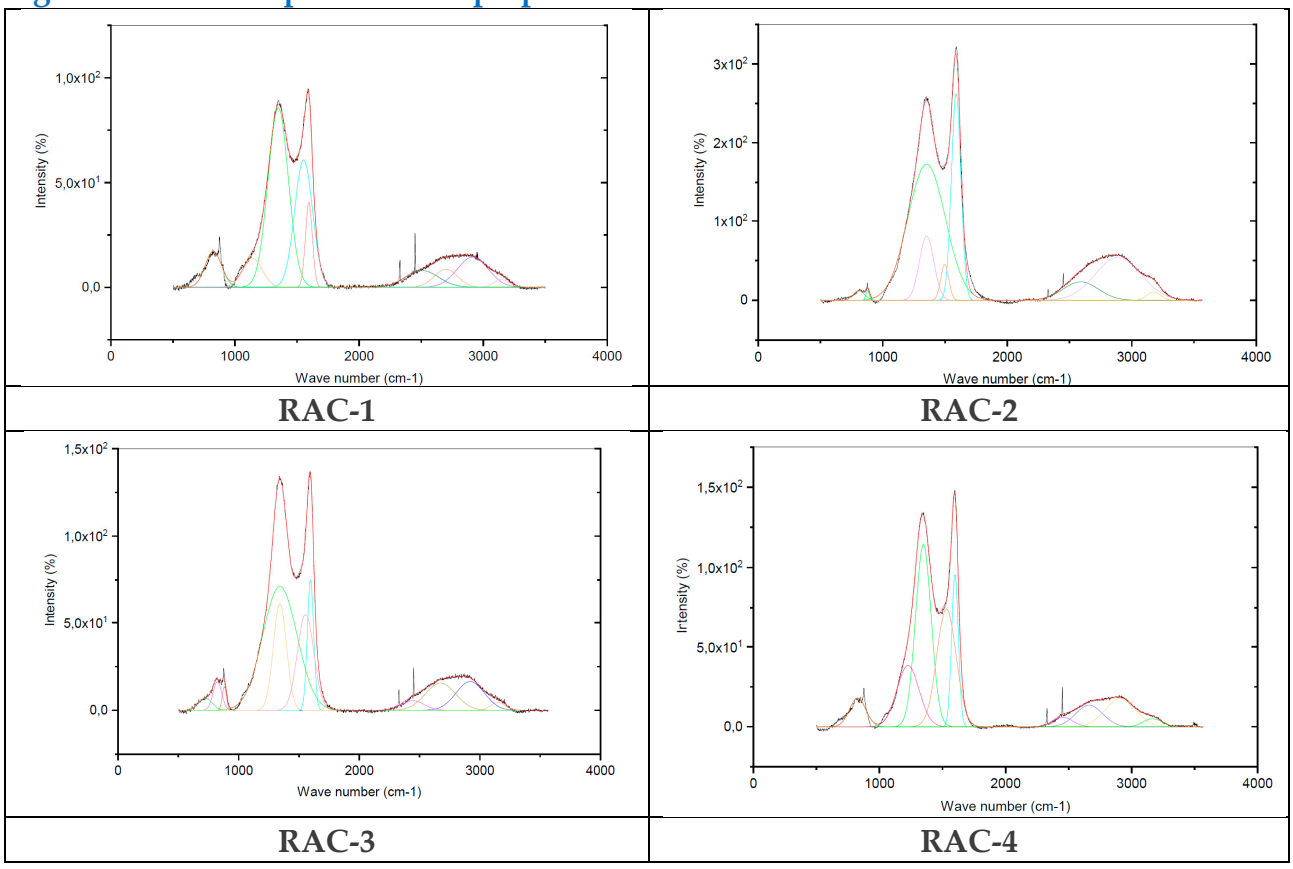

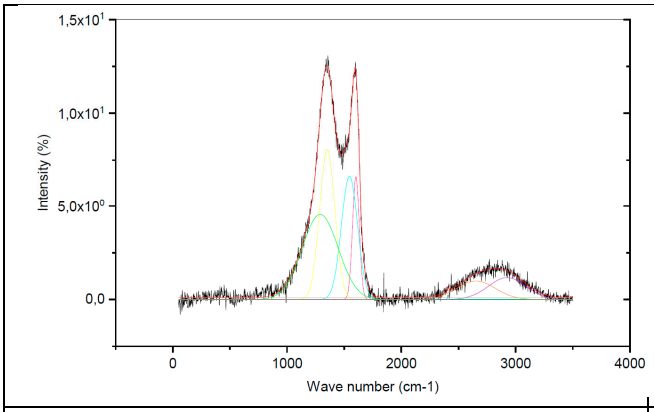

AAC-1

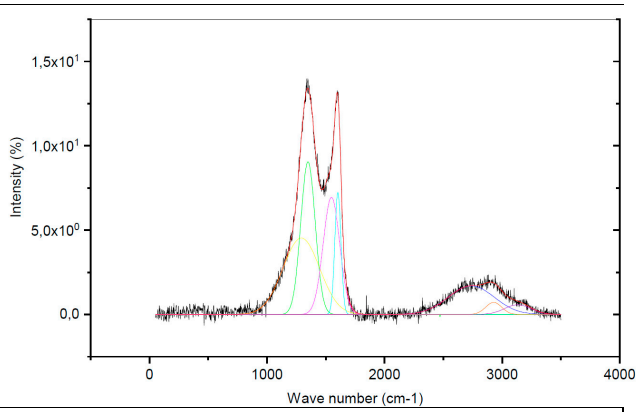

AAC-2

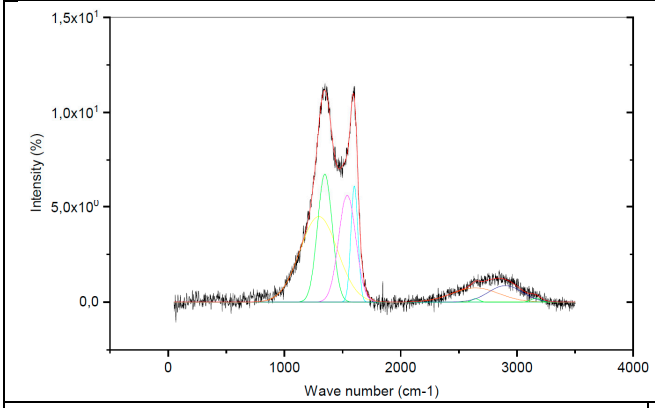

AAC-3

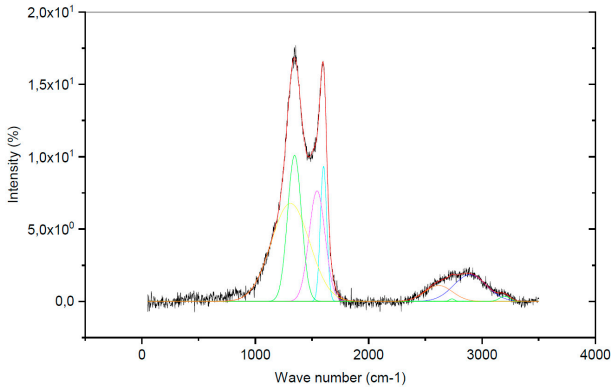

AAC-4

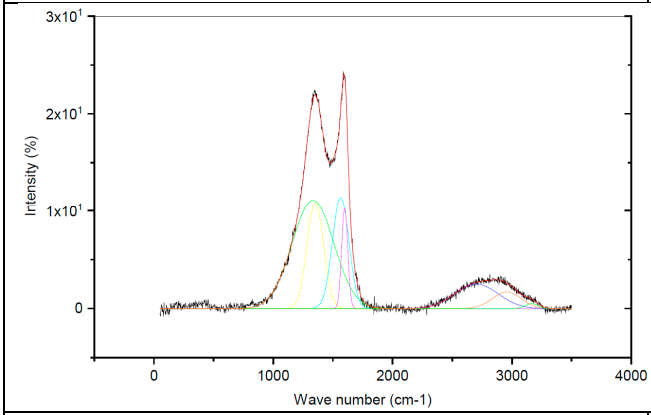

AAC-5

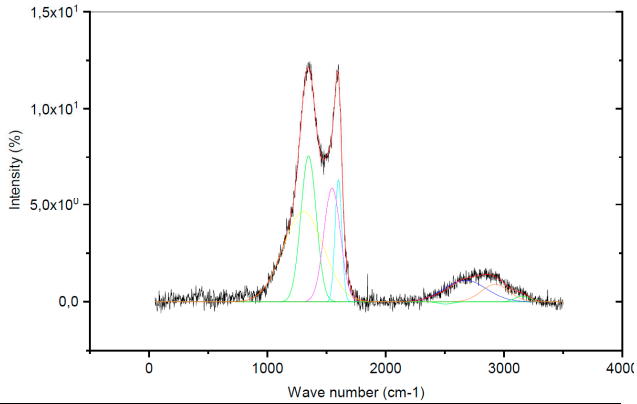

AAC-7

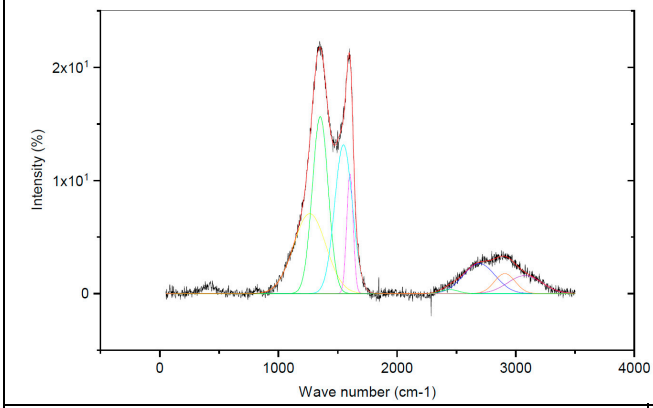

AAC-8

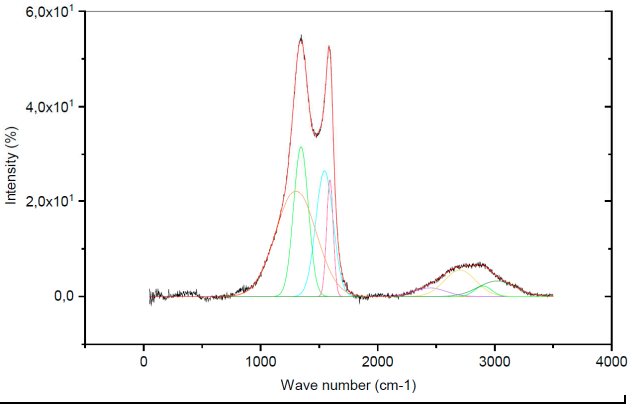

AAC-9

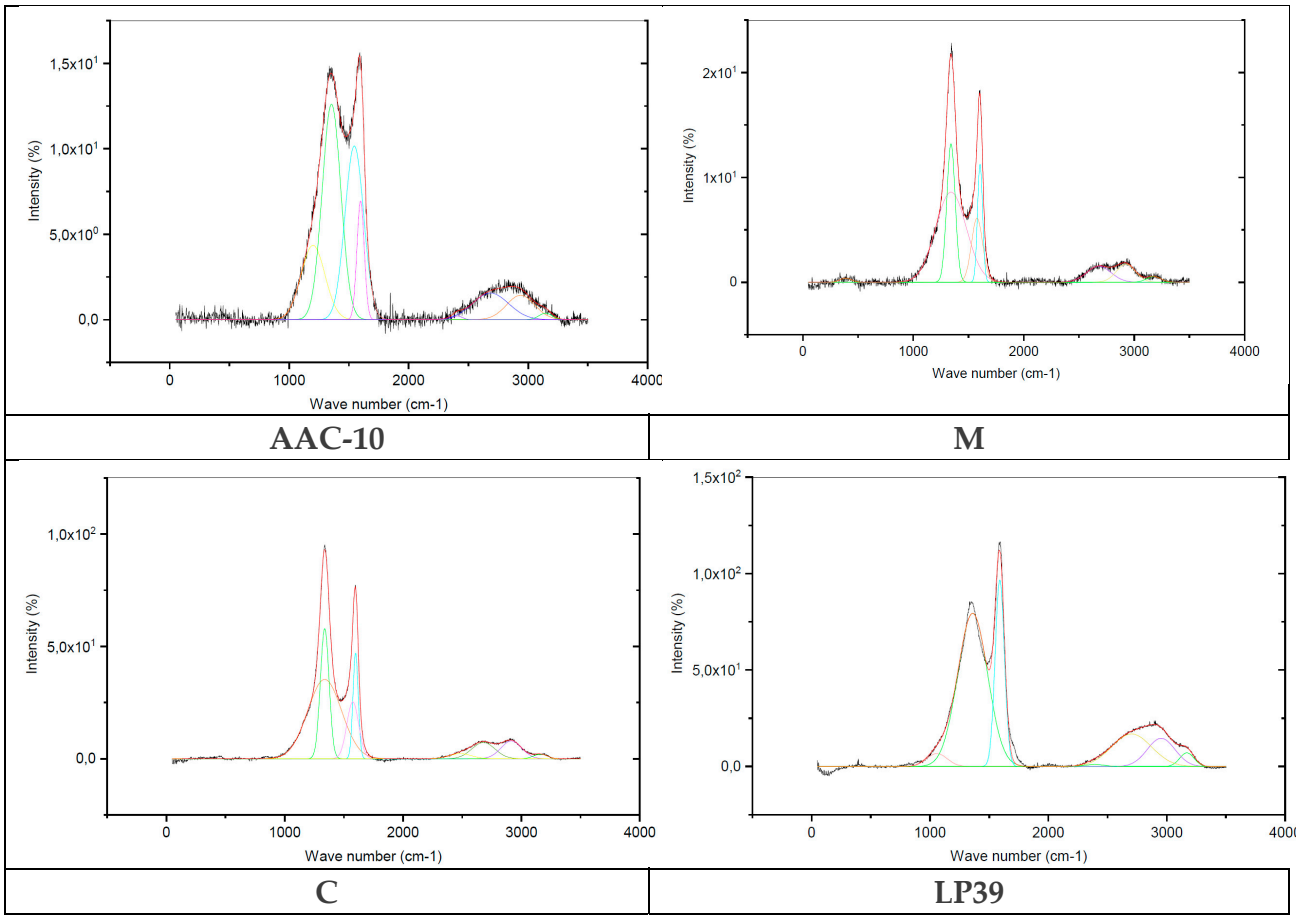

Figure S7. XRD spectra.

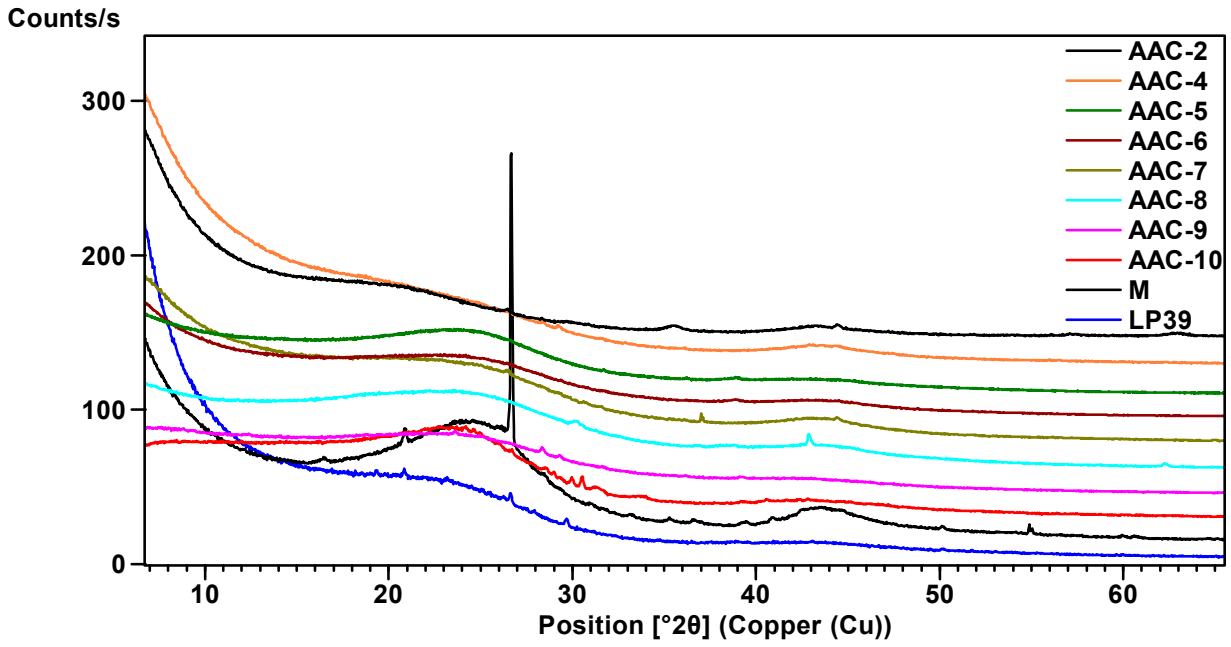

Figure S8. XPS spectra: (a) C 1s signal; (b) O 1s signal; (c) N 1s signal.

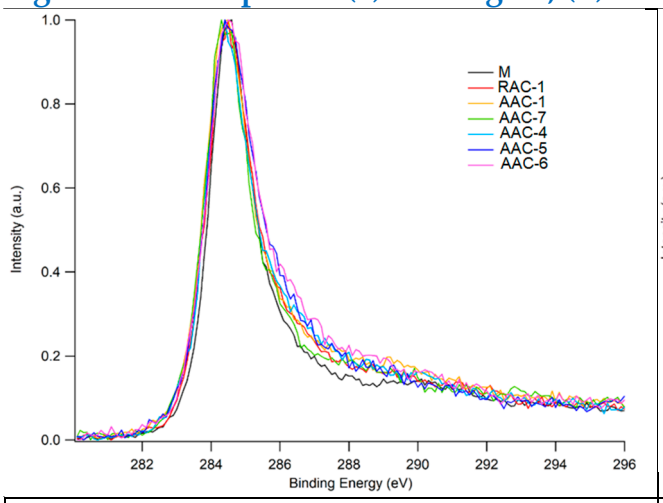

(a)

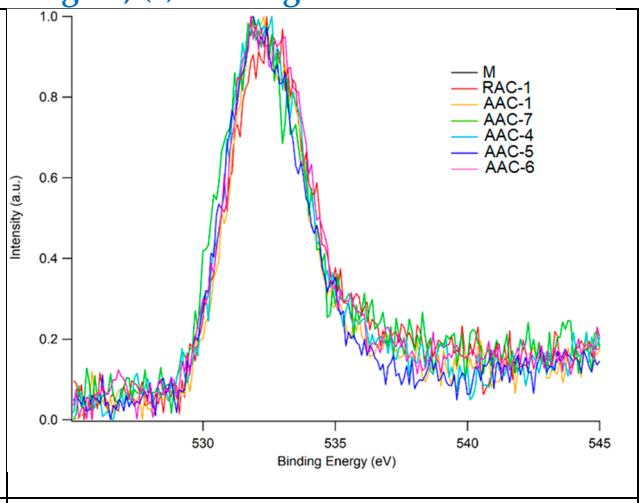

(b)

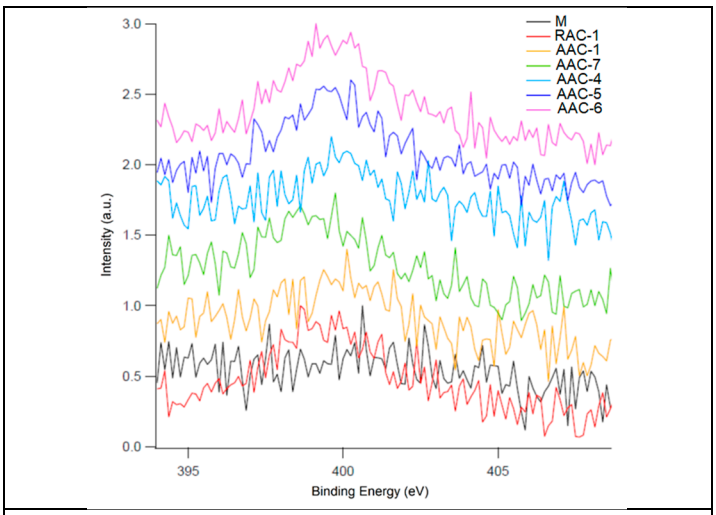

(c)

Figure S9. Selected ^{13}C NMR spectra in the solid state of the prepared AC.

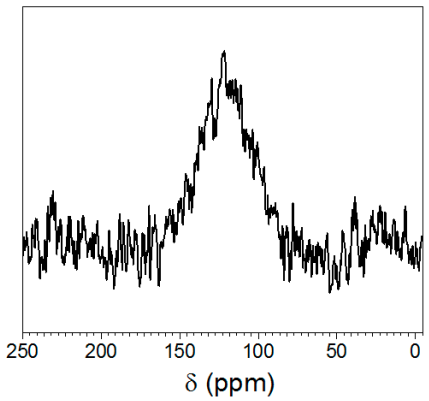

^{13}C MAS sample **AAC-4,** 12kHz
δ=121

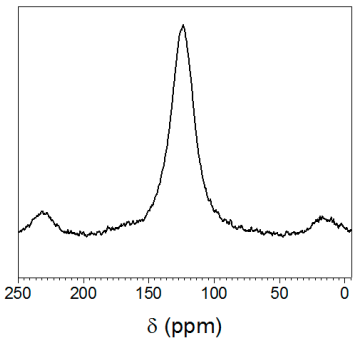

^{13}C CP-MAS sample **AAC-6,** 8kHz, D1=3s
δ= 124 ppm

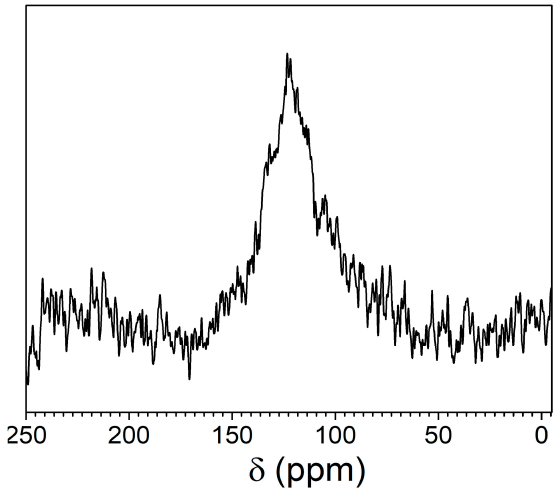	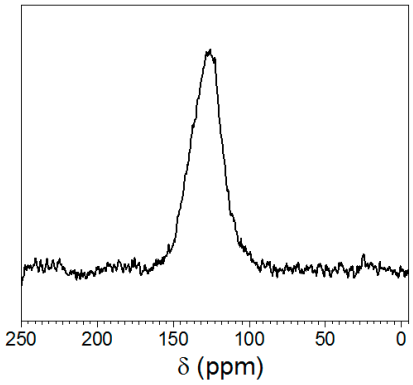
^{13}C MAS sample **AAC-9**, 10kHz, without ^{1}H-^{13}C dipolar decoupling δ=125 ppm	^{13}C MAS sample **AAC-10,** 10kHz δ=126 ppm
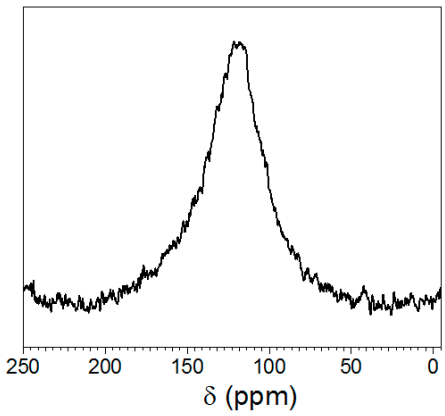	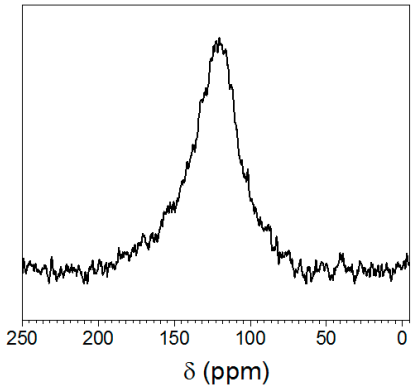
^{13}C MAS commercial sample **C,** 10kHz, without ^{1}H-^{13}C dipolar decoupling δ=120 ppm	^{13}C MAS commercial sample **M,** 10kHz, without ^{1}H-^{13}C dipolar decoupling δ=120 ppm
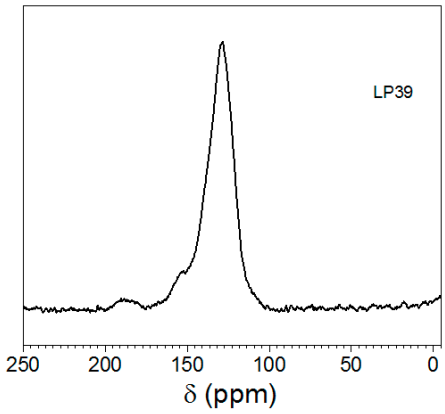	
^{13}C CP-MAS commercial sample **LP39,** 10kHz, D1=2s δ= 128, 153 (shoulder), 187 ppm	

Table S3. Parameters obtained from fitting two Gaussians as G and D bands to the Raman spectra of the ACs sample.

Sample	G band			D band			I_D/I_G
	Position (cm^{-1})	FWHM (cm^{-1})	Area	Position (cm^{-1})	FWHM (cm^{-1})	Area	
RAC-1	1584	88	138	1353	323	202	1,46
RAC-2	1587	85	286	1350	314	766	2,68
RAC-3	1586	83	143	1345	259	285	1,99
RAC-4	1591	74	205	1343	271	262	1,28
AAC-1	1588	87	166	1351	260	315	1,90
AAC-2	1590	86	203	1349	237	316	1,56
AAC-3	1588	84	143	1350	365	445	2,55
AAC-4	1590	85	201	1349	268	422	2,10
AAC-5	1589	87	262	1353	312	668	2,55
AAC-6	1588	87	182	1351	301	365	2,00
AAC-7	1587	85	147	1348	266	279	1,90
AAC-8	1590	97	317	1352	265	586	1,85
AAC-9	1580	87	671	1346	279	1039	1,55
AAC-10	1585	94	204	1354	339	355	1,74
Sample **M**	1597	69	141	1341	152	424	3,00
Sample **C**	1592	67	578	1337	147	1794	3,10
Sample **LP39**	1588	80	946	1350	239	2654	2,81

All the values have been obtained from the average of three measurements in different samples of each carbon.

Table S4. Parameters in ACs samples obtained from fitting four Gaussians G1, G2, D1 and D2 to the Raman spectra in the region 1000-1600 cm^{-1}.

Sample	G1		G2		D1		D2		I_{D1}/I_{G1}	I_{D2}/I_{G2}	I_{G2}/I_{G1}
	ν (cm^{-1})	ν (cm^{-1})	ν (cm^{-1})	ν (cm^{-1})	ν (cm^{-1})	ν (cm^{-1})	ν (cm^{-1})	ν (cm^{-1})			
RAC-1	1595	66	1552	170	1348	154	1140	192	6.20	0.25	3.88
RAC-2	1589	70	1497	175	1352	136	1350	352	2.59	3.26	0.14
RAC-3	1596	63	1555	169	1342	127	1338	333	5.17	0.89	1.91
RAC-4	1599	63	1531	179	1348	146	1226	207	2.79	0.60	2.22
AAC-1	1602	69	1546	165	1351	157	1289	372	2.78	1.54	2.41
AAC-2	1602	61	1548	166	1349	144	1292	367	2.94	1.44	2.59
AAC-3	1601	69	1540	171	1348	147	1296	379	2.80	2.30	2.25
AAC-4	1602	66	1545	166	1347	144	1310	398	2.35	2.12	2.04
AAC-5	1598	61	1565	161	1353	161	1333	408	2.84	2.46	2.99
AAC-6	1593	75	1562	162	1349	184	1277	256	2.22	1.69	2.40
AAC-7	1600	65	1547	163	1348	152	1303	402	2.75	1.94	2.29
AAC-8	1603	65	1546	168	1353	157	1264	319	1.84	0.98	3.44
AAC-9	1592	66	1545	174	1344	147	1301	406	2.87	1.93	2.88
AAC-10	1598	72	1545	183	1354	183	1199	234	4.62	0.55	3.73
M	1604	54	1576	124	1342	89	1340	295	1.96	3.85	1.21
C	1602	53	1571	138	1338	86	1338	336	2.04	3.98	1.22
LP39	1590	92	-	-	1361	297	-	-	2.65	-	-

All the values have been obtained from the average of three measurements in different samples of each carbon.

Table S5. Parameters in ACs samples obtained from fitting four Gaussians G*, G'', D+D' and 2D' to the Raman spectra in the region 2300-3200 cm^{-1}.

Sample	G*		G''		D+D'		2D'	
	ν (cm^{-1})	ν (cm^{-1})	ν (cm^{-1})	ν (cm^{-1})	ν (cm^{-1})	ν (cm^{-1})	ν (cm^{-1})	ν (cm^{-1})
RAC-1	2506	314	2699	219	2915	292	3147	147
RAC-2	-	-	2590	334	2890	432	3178	130
RAC-3	2444	220	2674	294	2920	275	3148	173
RAC-4	2454	183	2664	250	2911	282	3166	172
AAC-1	2408	12	2653	398	2925	387	-	-
AAC-2	2471	4	2737	458	2928	160	3133	263
AAC-3	-	-	2643	76	2901	342	3161	100
AAC-4	2617	287	2735	52	2894	341	3200	110
AAC-5	-	-	2703	425	2957	283	3165	126
AAC-6	2622	314	-	-	2879	360	-	-
AAC-7	2505	137	2672	422	2924	278	3153	146
AAC-8	2444	172	2692	317	2908	205	3077	339
AAC-9	2447	316	2704	315	2902	172	3020	377
AAC-10	2407	97	2684	357	2937	277	3145	130
M	-	-	2679	258	2925	202	3177	150
C	2484	218	2679	229	2914	206	3159	137
LP39	2390	190	2702	397	2952	274	3169	143

All the values have been obtained from the average of three measurements in different samples of each carbon.

Table S6. Elemental composition (% w/w) of the ACs from XPS data compared with elemental analysis and EDX data.

Sample	XPS			ESEM - EDX		Elemental Analysis		
	C	O	N	C	O	C	H	N
RAC-1	80.52	15.8	1.0	82.5	16.9	81.52	1.72	3.12
RAC-2	86.51	10.9	-	87.8	11.6	86.92	1.16	1.08
RAC-3	88.05	10.1	-	89.9	9.6	89.16	1.84	1.46
RAC-4	91.89	5.1	-	93.0	4.8	92.57	1.02	1.02
AAC-1	86.5	12.9	0.6	85.3	13.8	86.85	0.44	1.20
AAC-2	84.8	15.3	-	83.4	15.5	81.54	0.49	0.67
AAC-3	89.9	10.2	-	88.3	10.7	89.19	0.56	0.27
AAC-4	85.3	14.2	0.6	86.5	13.6	86.82	0.44	0.89
AAC-5	81.0	17.0	2.0	80.4	17.5	79.36	1.72	2.07
AAC-6	84.2	14.5	1.3	83.7	15.7	82.48	1.59	1.30
AAC-7	87.3	12.0	0.7	86.2	13.4	85.21	1.42	0.78
AAC-8	71.3	28.7	-	72.7	27.0	72.33	0.88	0.37
AAC-9	85.3	14.6	-	84.8	15.0	85.42	0.52	0.64
AAC-10	80.4	19.6	-	79.6	20.0	80.12	0.92	0.48
M	90.2	7.8	0.3	92.4	6.7	91.8	0.98	0.51
C	92.6	6.6	-	94.0	5.6	93.1	0.37	-
LP39	84.9	10.2	-	86.9	11.5	85.2	0.50	-

Figure S10. Selected N_2 absorption isotherm profiles together with pore size distribution.

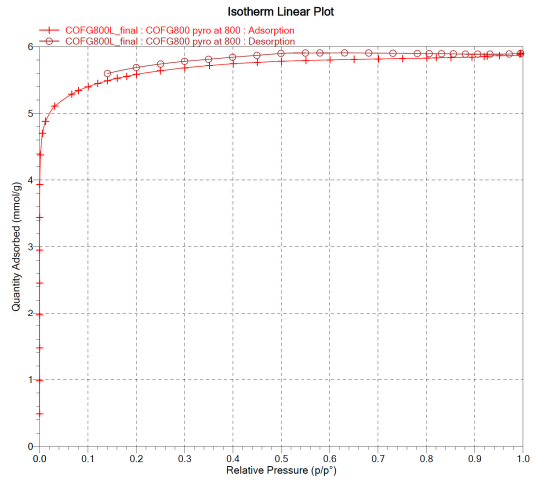

N_2 absorption isotherm of **RAC-3** (BET 478 m^2/g)

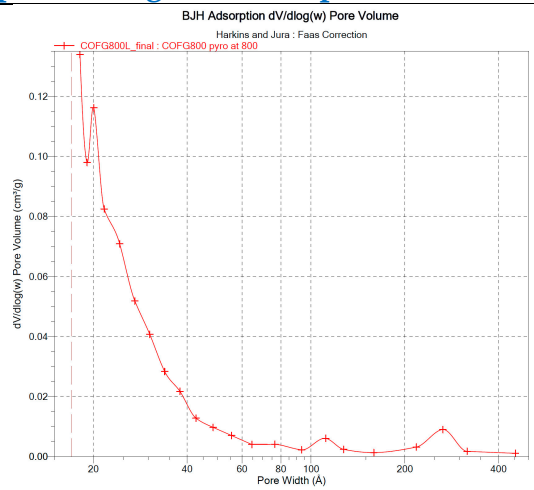

Pore size distribution for **RAC-3**

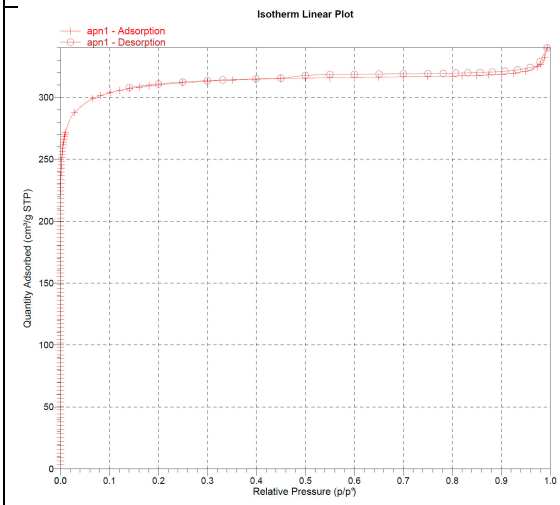

N_2 absorption isotherm of **AAC-9** (BET 1200 m^2/g)

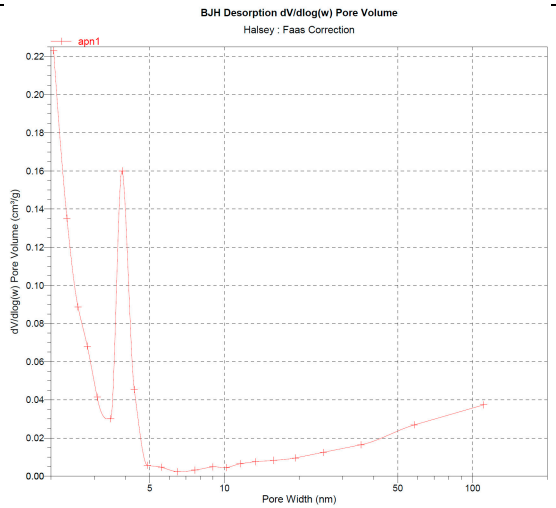

Pore size distribution for **AAC-9**

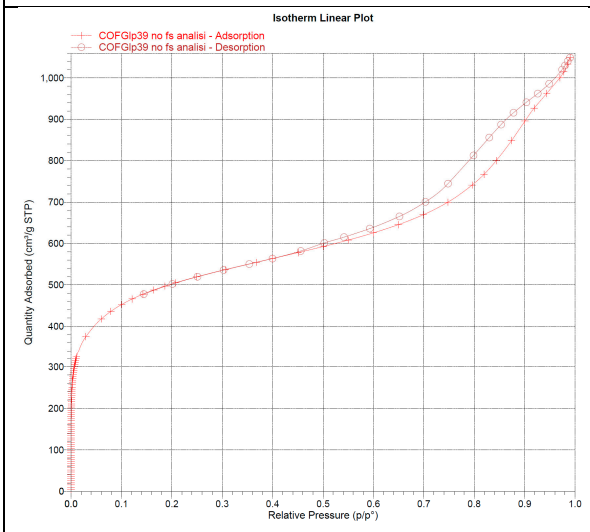

N_2 absorption isotherm of commercial **LP39** (BET 1782 m^2/g)

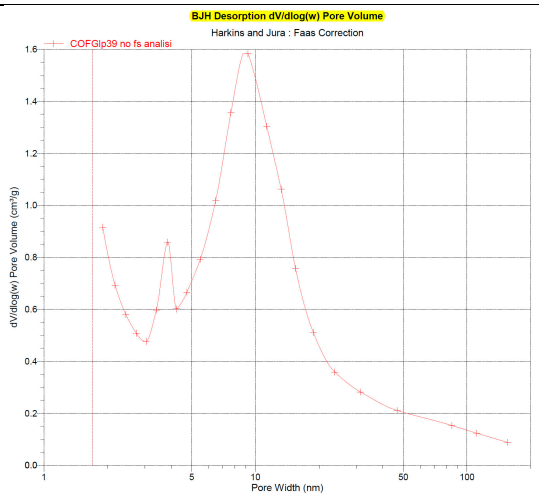

Pore size distribution for commercial **LP39**

Figure S11. ESEM images of the activated carbons at different magnifications.

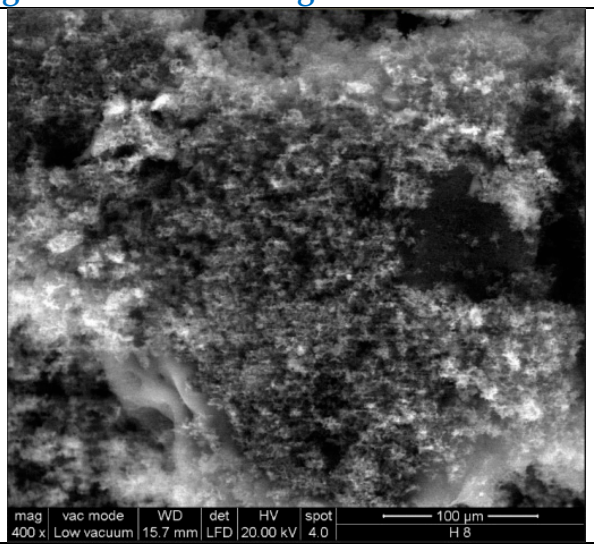

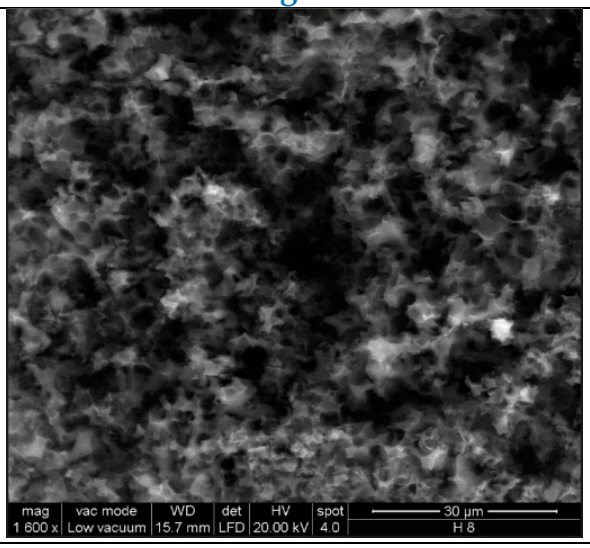

RAC-1

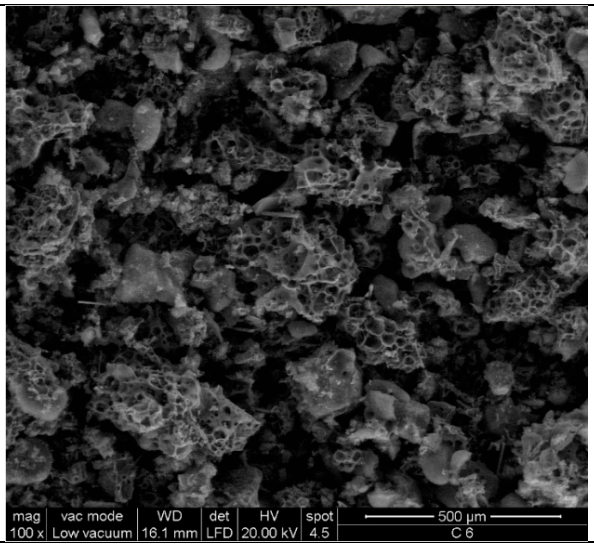

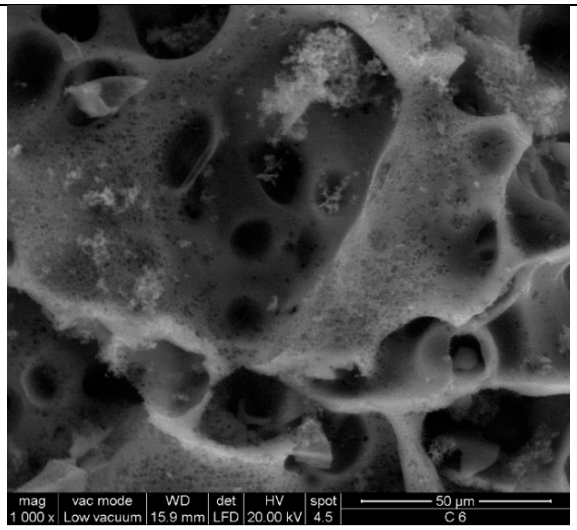

RAC-2

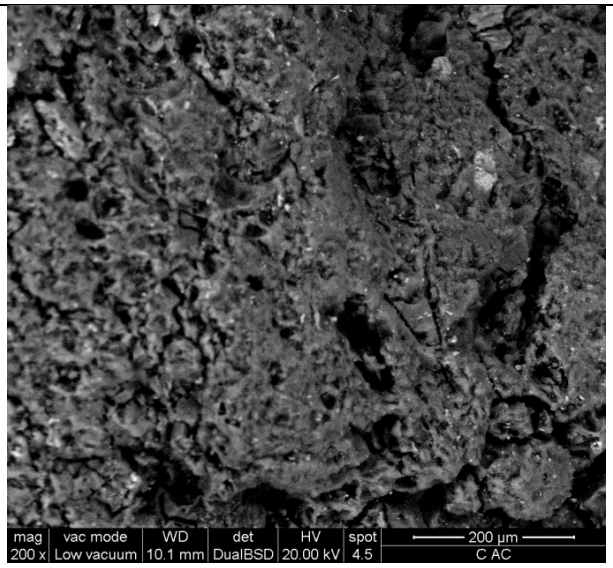

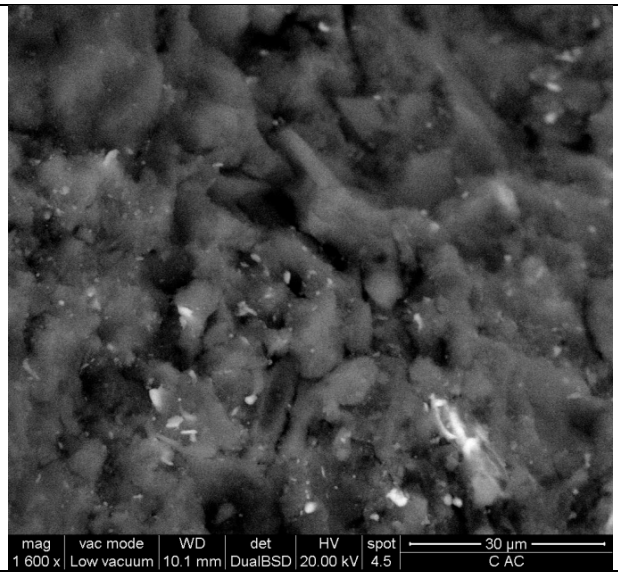

RAC-3

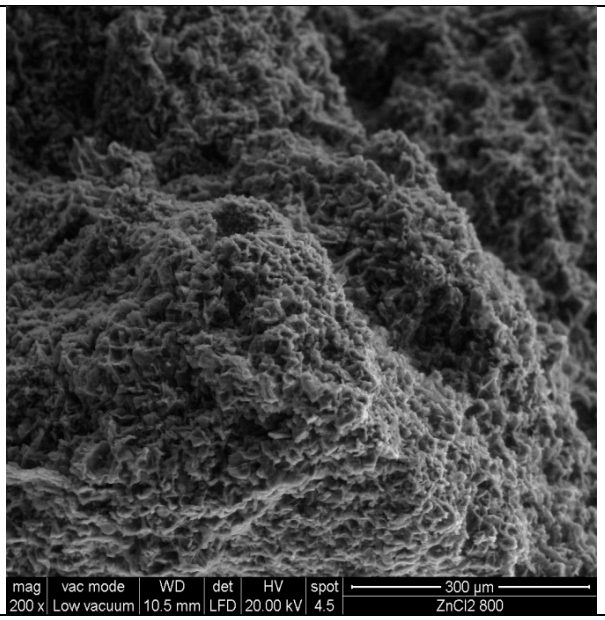

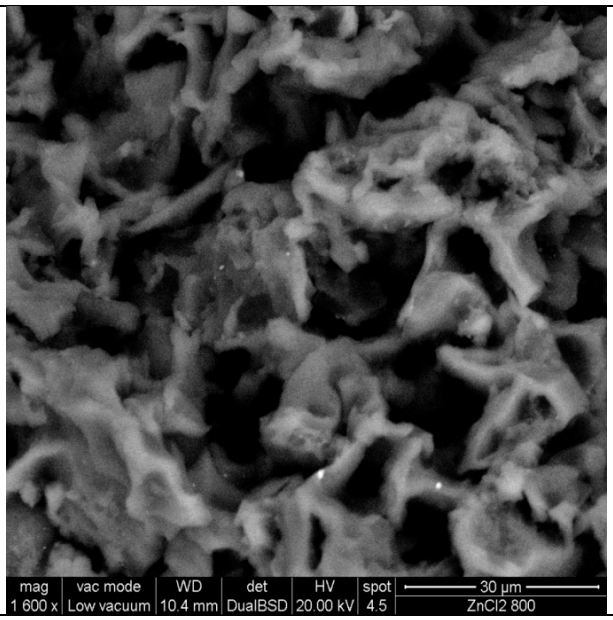

RAC-4

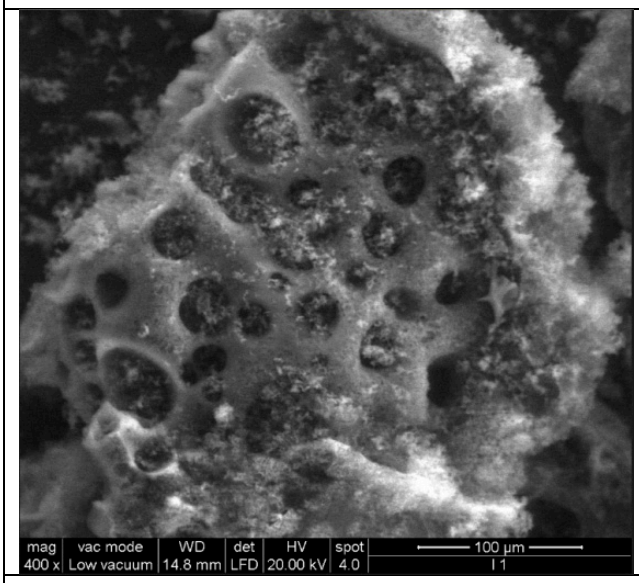

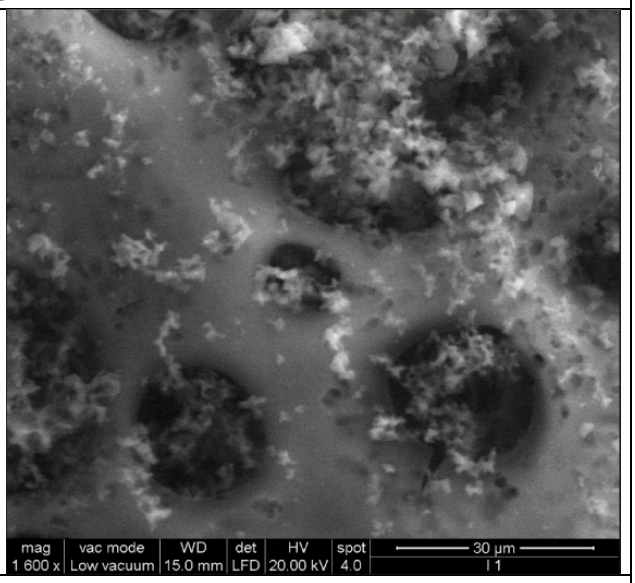

AAC-1

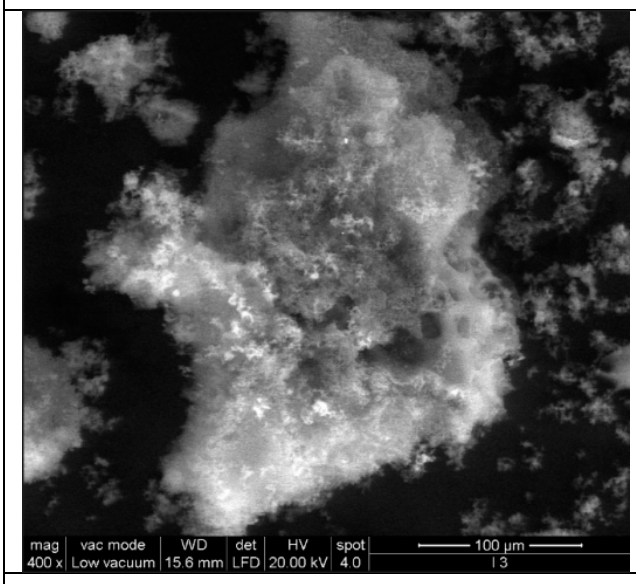

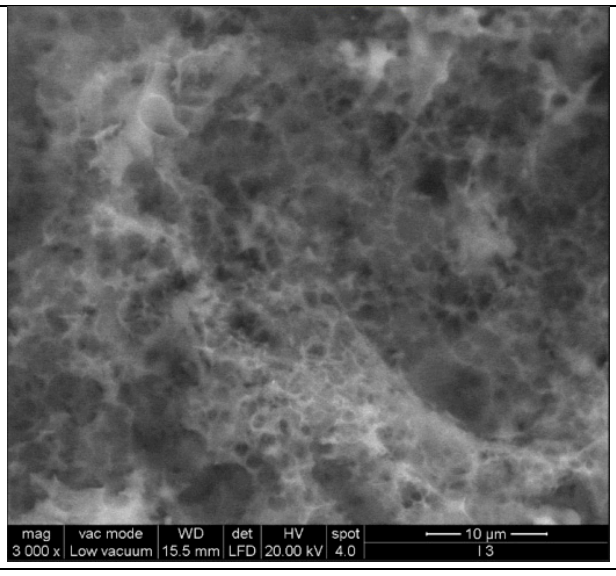

AAC-2

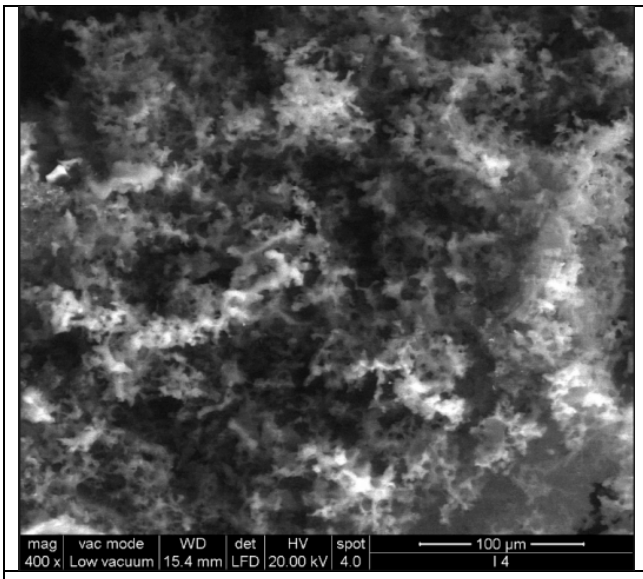

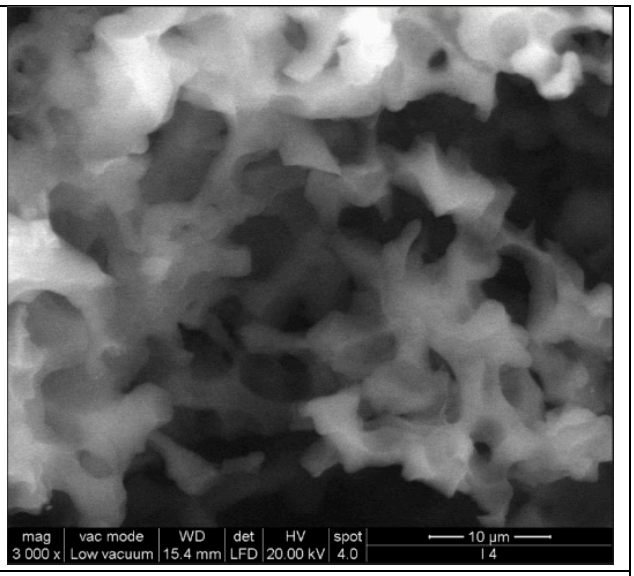

AAC-3

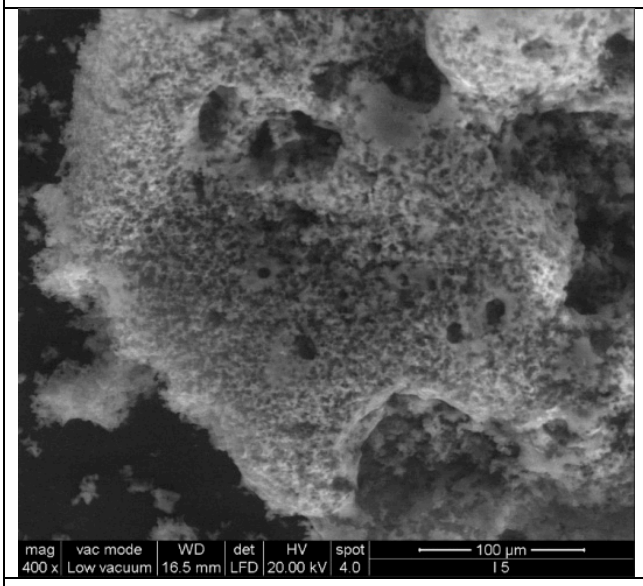

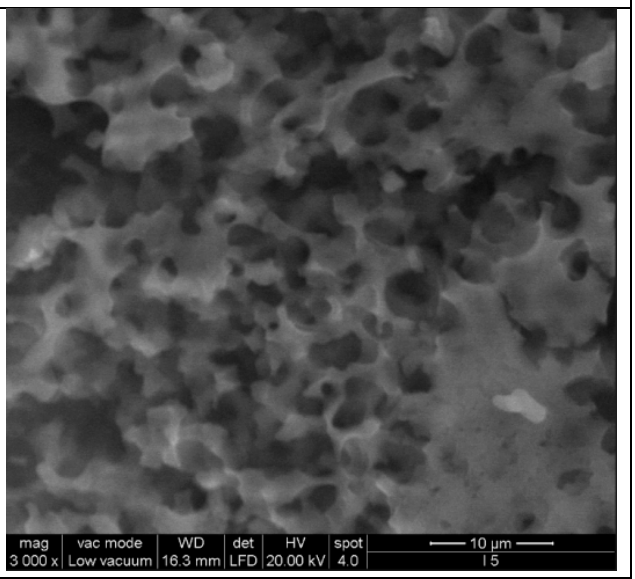

AAC-4

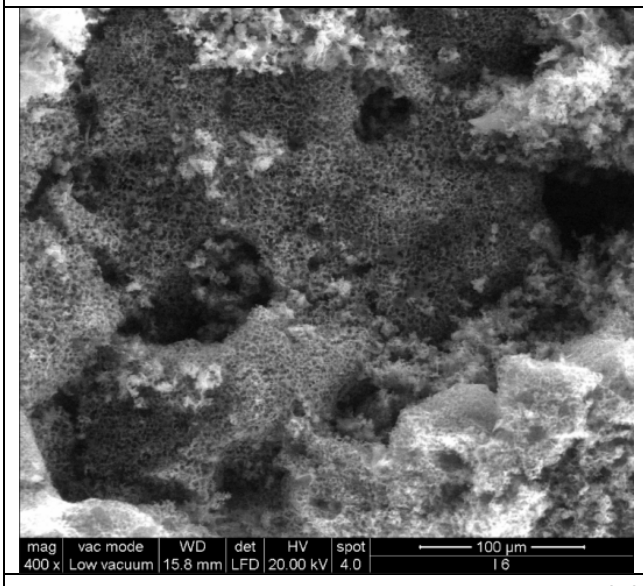

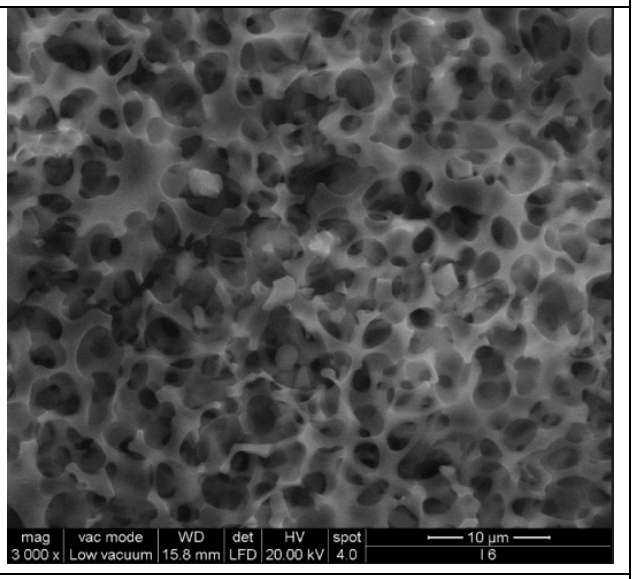

AAC-5

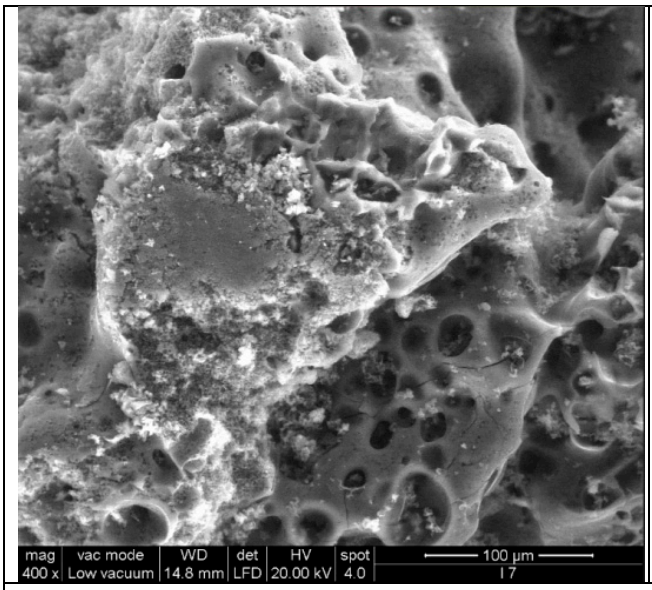

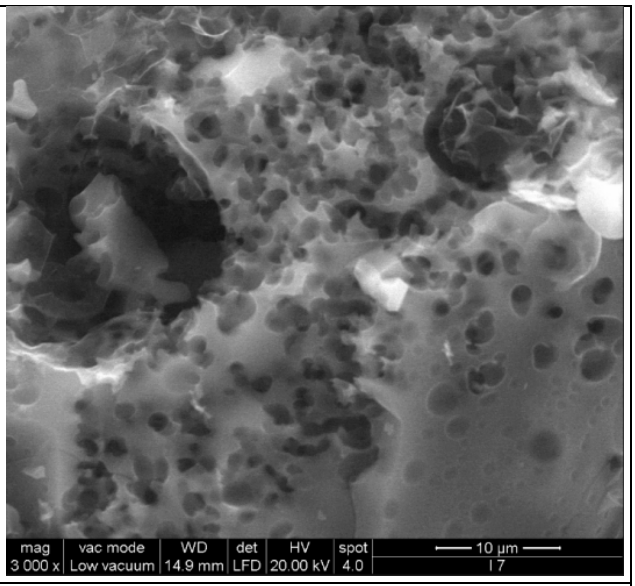

AAC-6

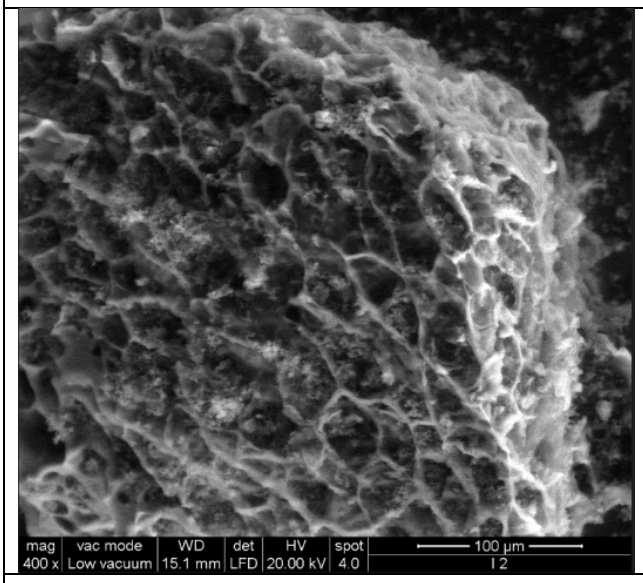

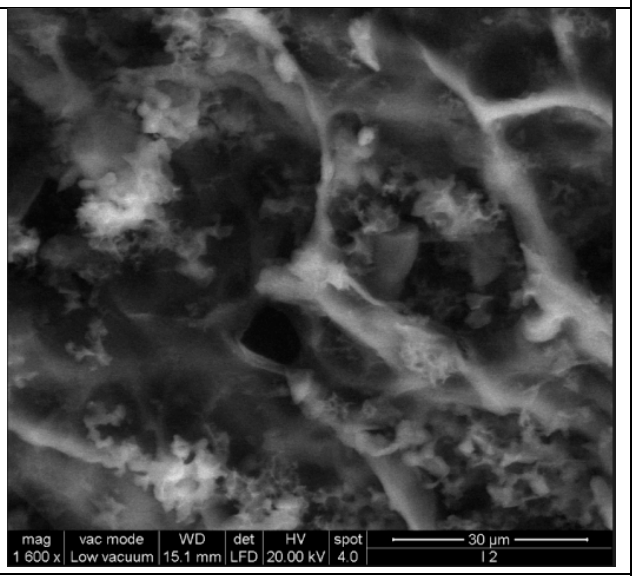

AAC-7

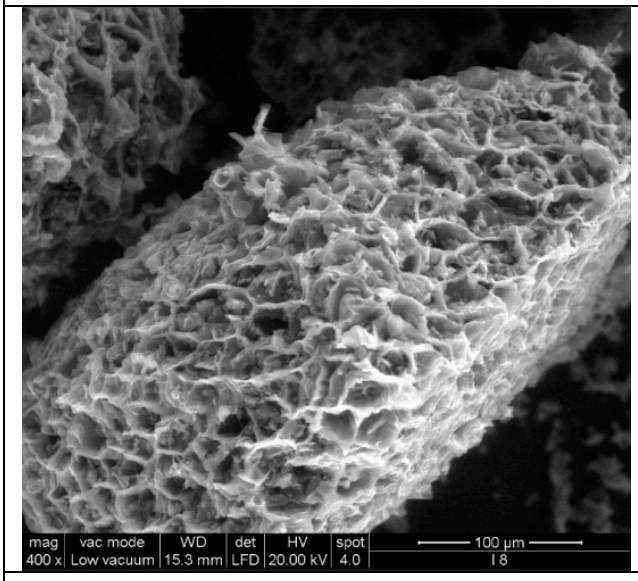

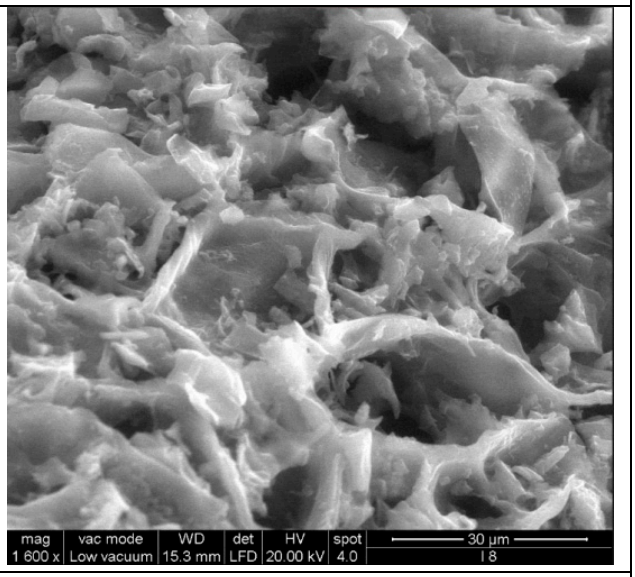

AAC-8

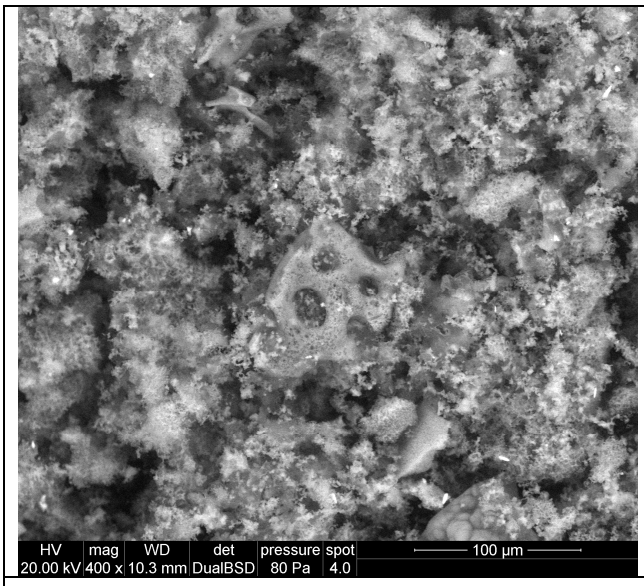
HV mag WD det pressure spot
20.00 kV 400 x 10.3 mm DualBSD 80 Pa 4.0
100 µm

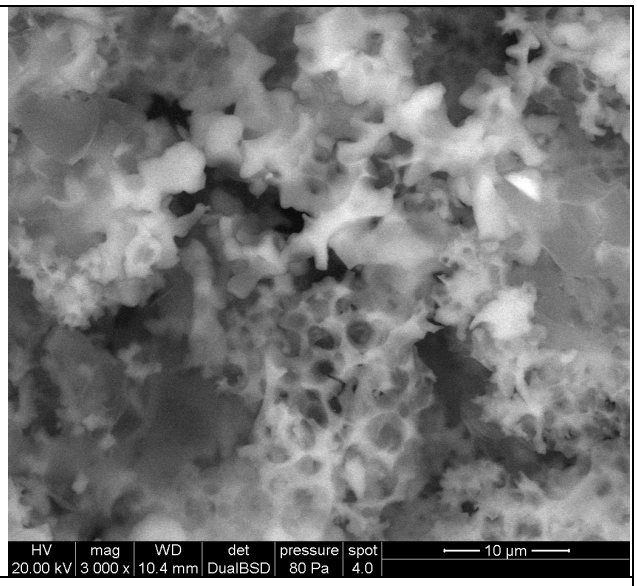
HV mag WD det pressure spot
20.00 kV 3 000 x 10.4 mm DualBSD 80 Pa 4.0
10 µm

AAC-9

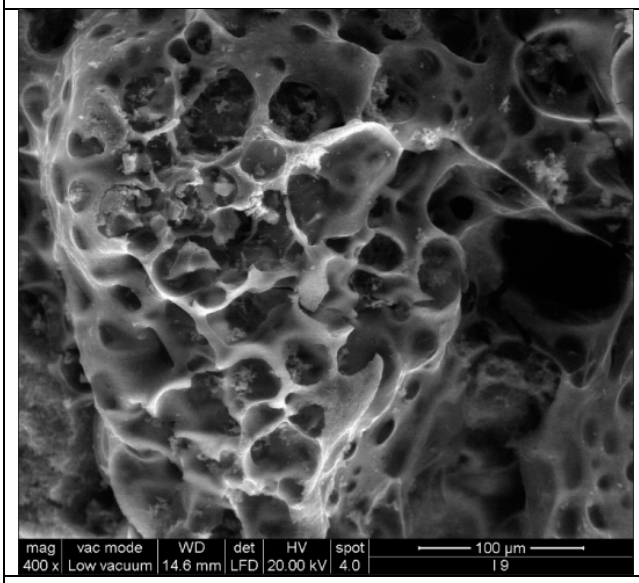
mag vac mode WD det HV spot
400 x Low vacuum 14.6 mm LFD 20.00 kV 4.0
100 µm
I 9

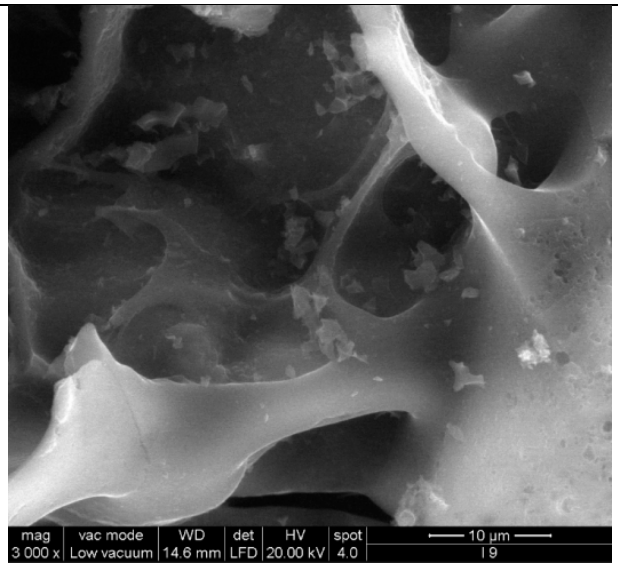
mag vac mode WD det HV spot
3 000 x Low vacuum 14.6 mm LFD 20.00 kV 4.0
10 µm
I 9

AAC-10

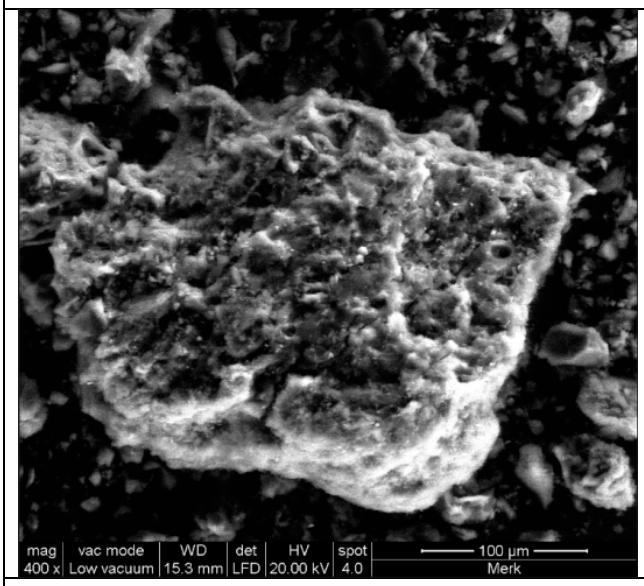
mag vac mode WD det HV spot
400 x Low vacuum 15.3 mm LFD 20.00 kV 4.0
100 µm
Merk

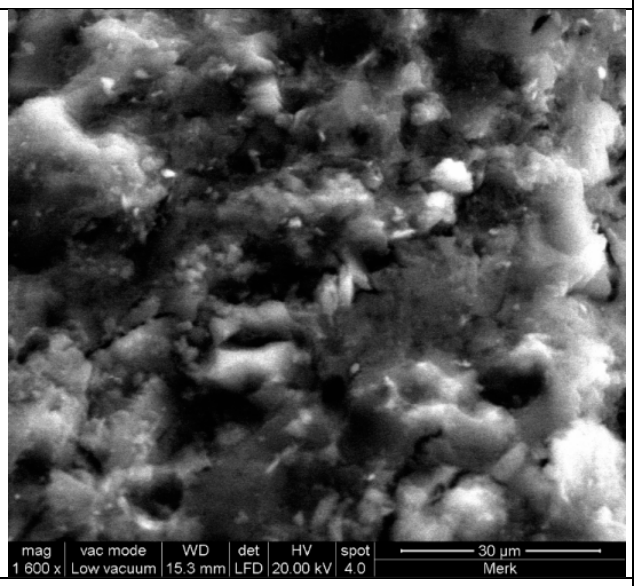
mag vac mode WD det HV spot
1 600 x Low vacuum 15.3 mm LFD 20.00 kV 4.0
30 µm
Merk

M

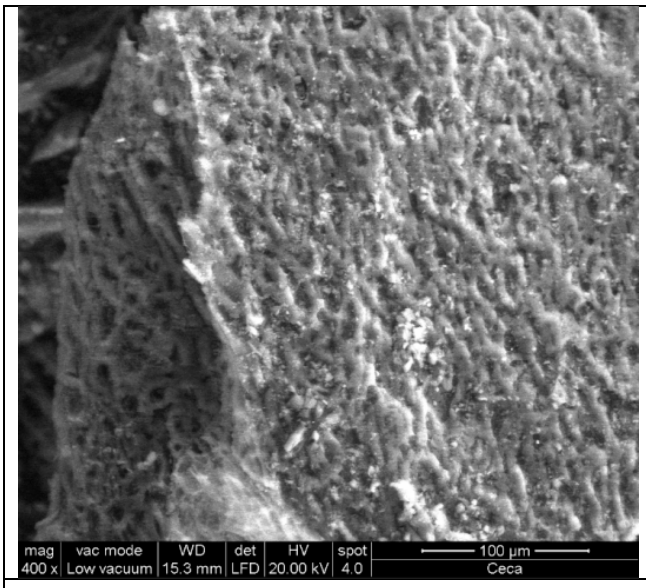
mag
400 x
vac mode
Low vacuum
WD
15.3 mm
det
LFD
HV
20.00 kV
spot
4.0
100 µm
Ceca

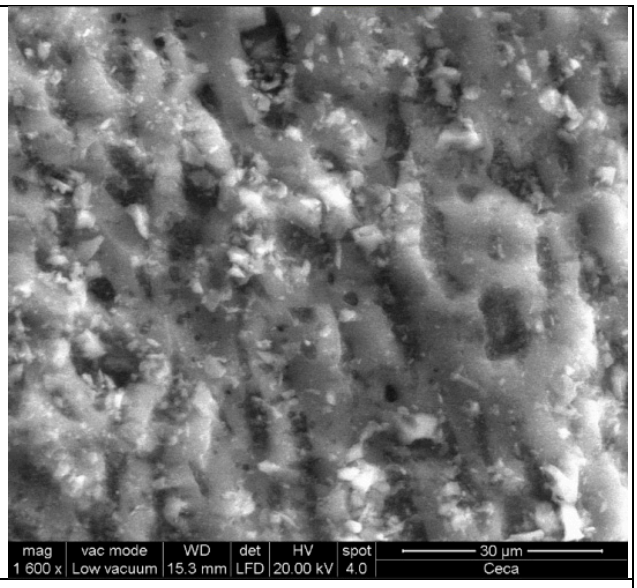
mag
1 600 x
vac mode
Low vacuum
WD
15.3 mm
det
LFD
HV
20.00 kV
spot
4.0
30 µm
Ceca

C

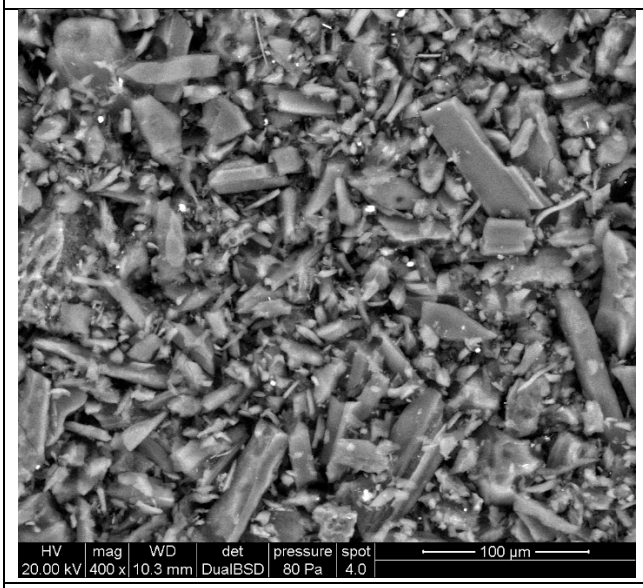
HV
20.00 kV
mag
400 x
WD
10.3 mm
det
DualBSD
pressure
80 Pa
spot
4.0
100 µm

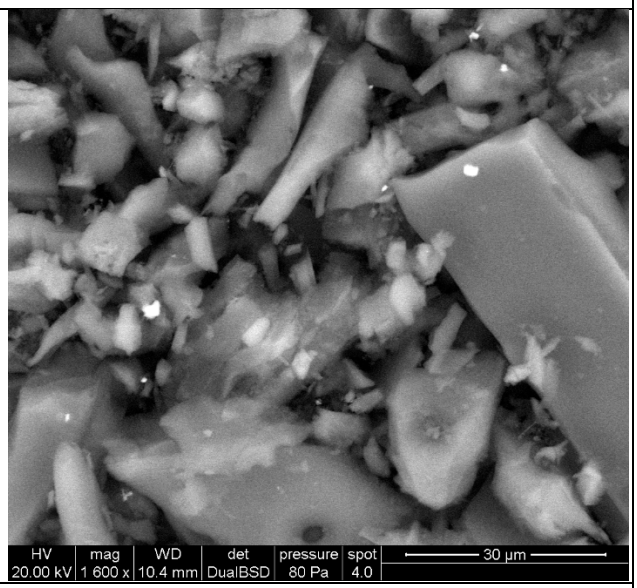
HV
20.00 kV
mag
1 600 x
WD
10.4 mm
det
DualBSD
pressure
80 Pa
spot
4.0
30 µm

LP39

Figure S12. TEM images of the samples AAC-5, AAC-6 and AAC-7, prepared by KOH activation at 600°C, 700°C, and 800°C, respectively.

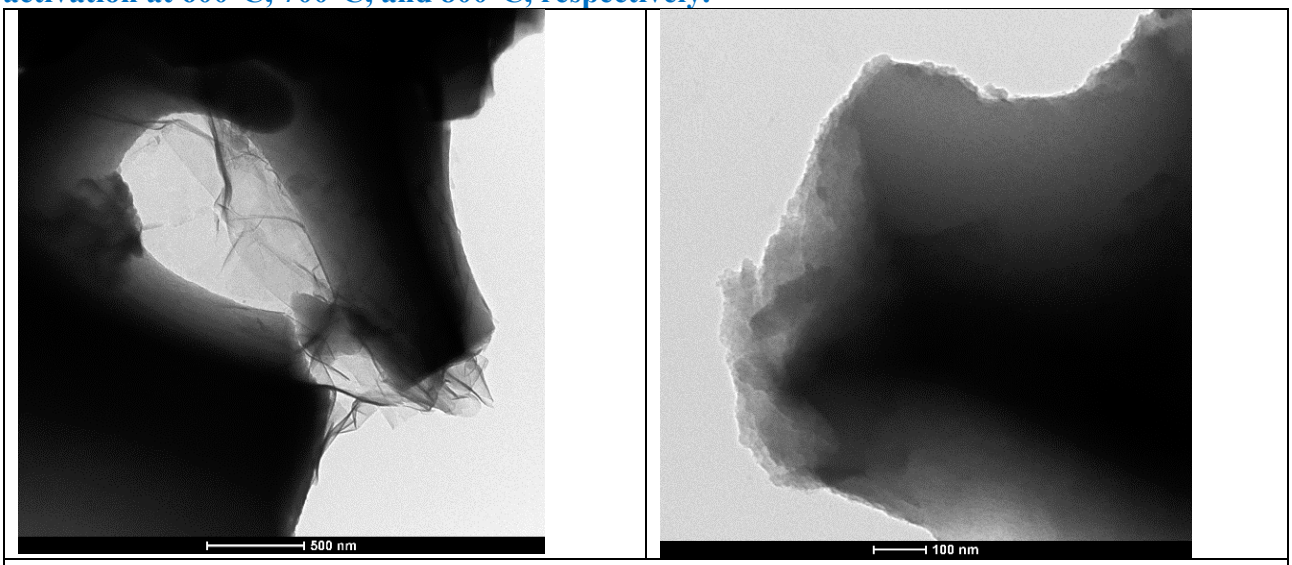

AAC-5

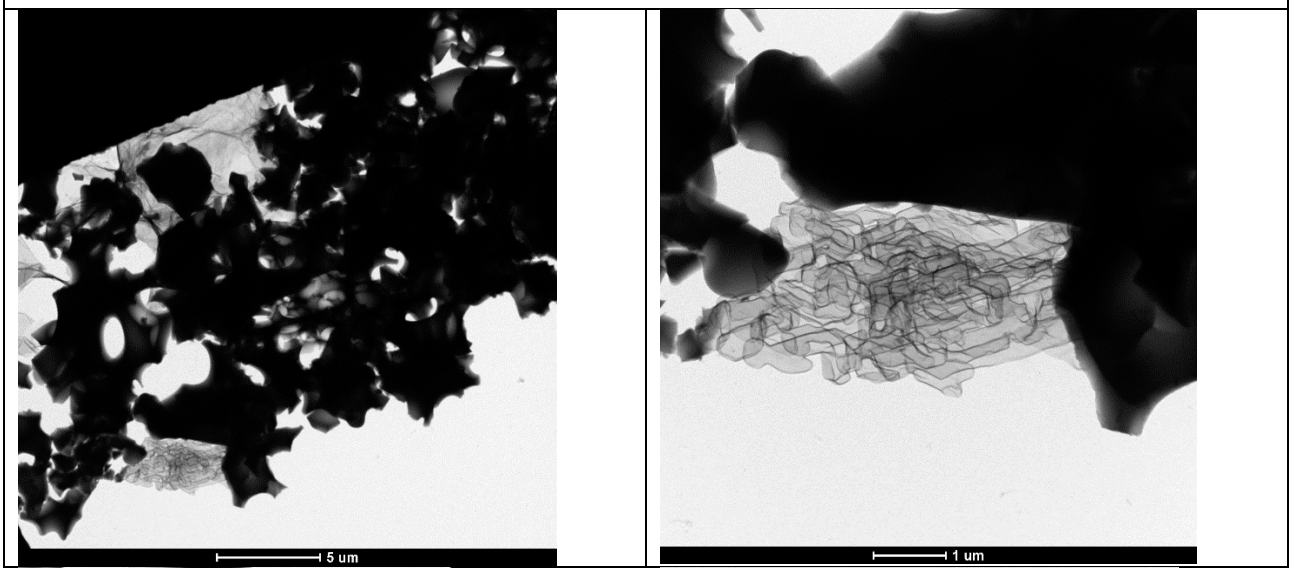

AAC-6

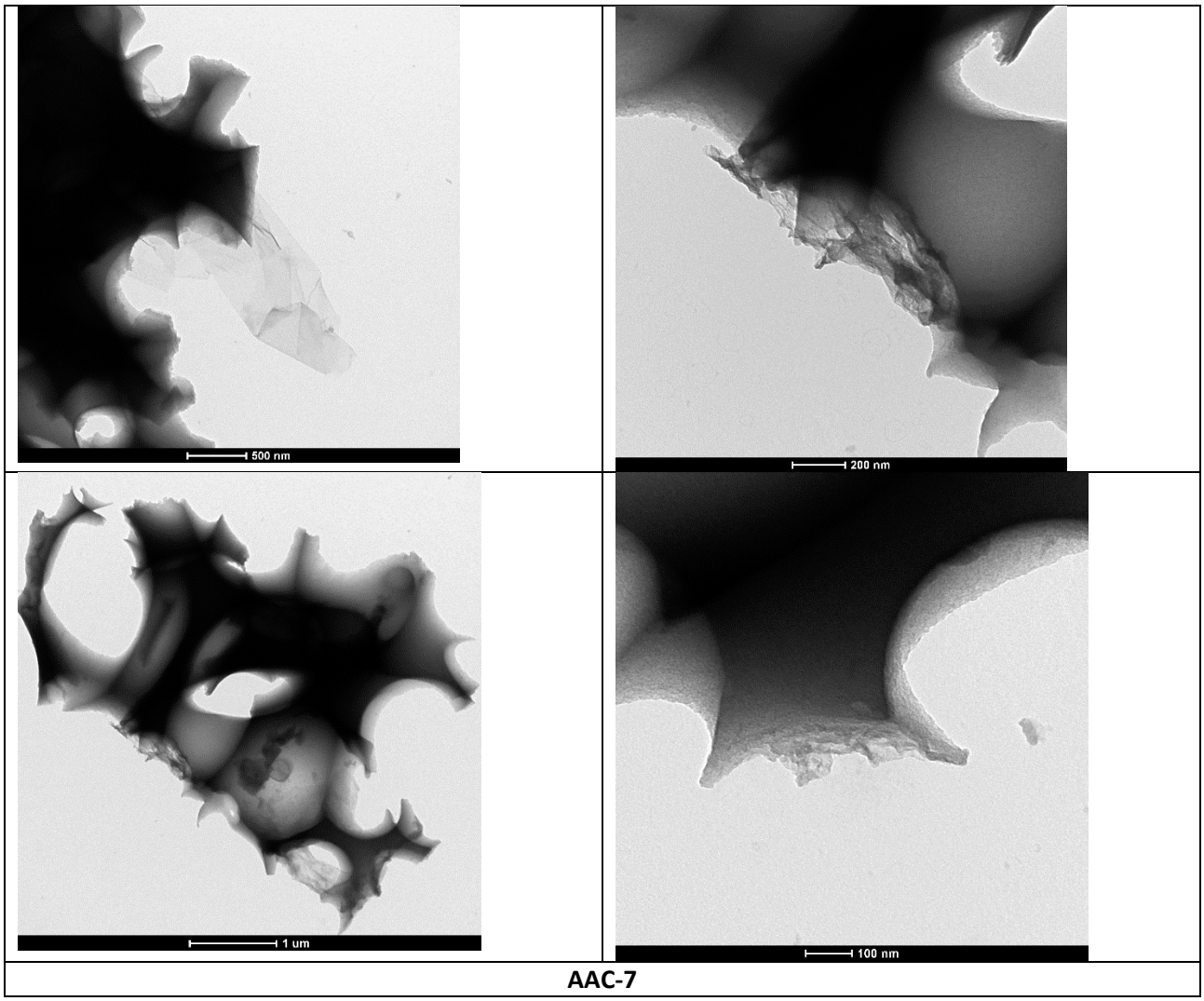

Figure S13. (a). Raman I_D/I_G ratio *vs* pore diameter for samples with BET values higher than 1000 m^2/g. (b). Raman I_D/I_G ratio *vs* pore diameter for samples with BET values lower than 1000 m^2/g.

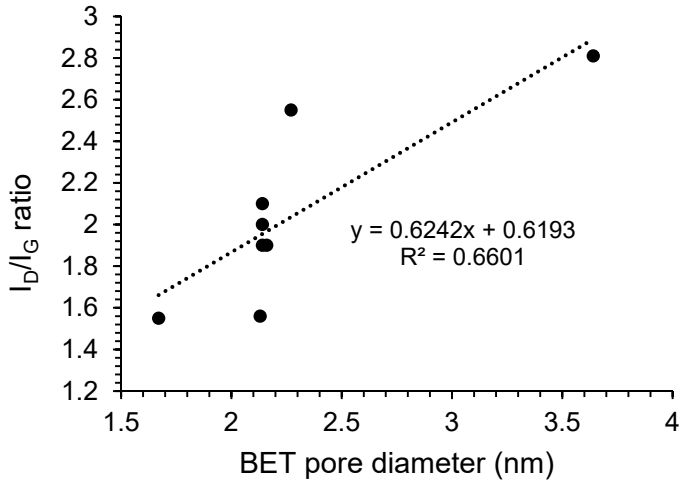

(**a**)

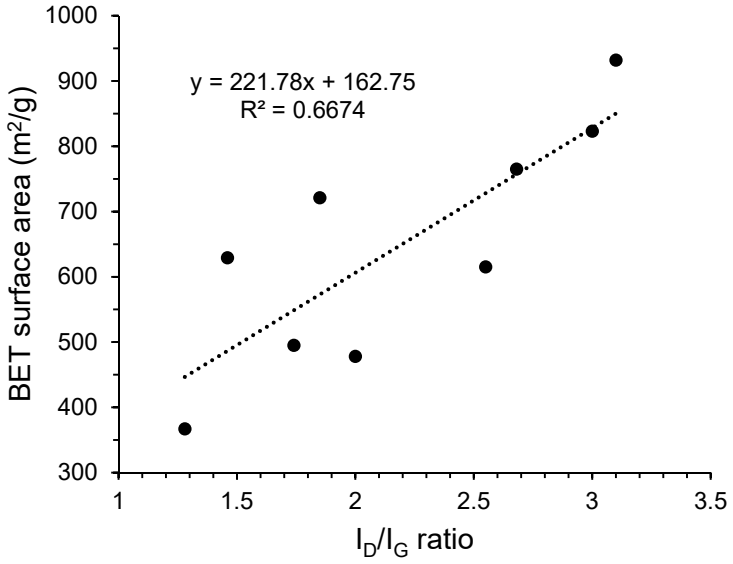

(**b**)

Figure S14: Raman I_D/I_G ratio *vs* specific surface area for samples with BET values higher than 1000 m^2/g.